

Phosphorus–Nitrogen Compounds. 21. Syntheses, Structural Investigations, Biological Activities, and DNA Interactions of New N/O Spirocyclic Phosphazene Derivatives. The NMR Behaviors of Chiral Phosphazenes with Stereogenic Centers upon the Addition of Chiral Solvating Agents

Muhammet Işıklan,[†] Nuran Asmafiliz,[‡] Ezgi Elif Özalp,[‡] Elif Ece İltir,[§] Zeynel Kılıç,^{*,‡} Bünyemin Çoşut,[‡] Serkan Yeşilot,[‡] Adem Kılıç,[‡] Aslı Öztürk,^{||} Tuncer Hökelek,[¶] L. Yasemin Koç Bilir,[□] Leyla Açık,[#] and Emel Akyüz[#]

[†]Department of Chemistry, Kırıkkale University, Kırıkkale, Turkey, [‡]Department of Chemistry, Ankara University, 06100 Ankara, Turkey, [§]TÜBİTAK, Scientific and Technical Research Council of Turkey, 06100 Ankara, Turkey, ^{||}Department of Chemistry, Gebze Institute of Technology, 41400 Kocaeli, Turkey, [¶]Department of Physics, Pamukkale University, Denizli, Turkey, [□]Department of Physics, Hacettepe University, 06800 Ankara, Turkey, [□]Department of Biology, Ankara University, 06100 Ankara, Turkey, and [#]Department of Biology, Gazi University, 06500 Ankara, Turkey

Received April 22, 2010

The reactions of hexachlorocyclotriphosphazatriene, $N_3P_3Cl_6$, with N/O-donor-type *N*-alkyl (or aryl)-*o*-hydroxybenzylamines (**1a–1e**) produce mono- (**2a–2e**), di- (**3a–3d**), and tri- (**4a** and **4b**) spirocyclic phosphazenes. The tetrapyrrolidino monospirocyclic phosphazenes (**2f–2i**) are prepared from the reactions of partly substituted compounds (**2a–2d**) with excess pyrrolidine. The dispirodipyrrolidinophosphazenes (**3e–3h**) and trispirophosphazenes (**3i–3k**) are obtained from the reactions of *trans*-dispirophosphazenes with excess pyrrolidine and sodium (3-amino-1-propanoxide), respectively. Compounds **3a–3d** have *cis* and *trans* geometric isomers. Only the *trans* isomers of these compounds are isolated. Compounds **3a–3h** have two stereogenic P atoms. They are expected to be in *cis* (meso) and *trans* (racemic) geometric isomers. In the *trans* trispiro compounds (**3i–3k**), there are three stereogenic P atoms. They are expected to be in racemic mixtures. The stereogenic properties of **3a–3k** are confirmed by ³¹P NMR spectroscopy upon the addition of the chiral solvating agent; (*S*)-(+)-2,2,2-trifluoro-1-(9'-anthryl)ethanol. The molecular structures of **3i–3k**, **4a**, and **4b** look similar to a propeller, where the chemical environment of one P atom is different from that of others. Additionally, **4a** and **4b** are also expected to exist as *cis–trans–trans* and *cis–cis–cis* geometric isomers, but both of them are found to be in *cis–trans–trans* geometries. The solid-state structures of **2a**, **2e**, **2f**, **3e**, and **3f** are determined by X-ray crystallography. The compounds **2f–2i**, **3e–3i**, and **3k** are screened for antibacterial activity against Gram-positive and Gram-negative bacteria and for antifungal activity against yeast strains. These compounds (except **3f**) have shown a strong affinity against most of the bacteria. Minimum inhibitory concentrations (MIC) are determined for **2f–2i**, **3e–3i**, and **3k**. DNA binding and the nature of interaction with pUC18 plasmid DNA are studied. The compounds **2f–2i**, **3e–3i**, and **3k** induce changes on the DNA mobility. The prevention of *Bam*HI and *Hind*III digestion (except **2g**) with compounds indicates that the compounds bind with nucleotides in DNA.

Introduction

In recent years, there has been a considerable amount of interest in the synthesis of spirocyclic phosphazenes in general and in the determination of the stereogenic properties of

chiral cyclophosphazenes in particular.¹ Reactions of bifunctional reagents with $N_3P_3Cl_6$ may lead to spiro, ansa, bino, dispiro, spiro-ansa, and trispirocyclophosphazenic derivatives.² Both functional groups of the ligand may be replaced with

*To whom correspondence should be addressed. E-mail: zkilic@science.ankara.edu.tr.

(1) (a) Chandrasekhar, V.; Krishnan, V. *Adv. Inorg. Chem.* **2002**, *53*, 159–211. (b) Bešli, S.; Coles, S. J.; Davies, D. B.; Eaton, R. J.; Hursthouse, M. B.; Kılıç, A.; Shaw, R. A.; Çiftçi, G. Y.; Yeşilot, Ş. *J. Am. Chem. Soc.* **2003**, *125*, 4943–4950. (c) Chandrasekhar, V.; Thilagar, P.; Pandian, B. M. *Coord. Chem. Rev.* **2007**, *251*, 1045–1074. (d) Coles, S. J.; Davies, D. B.; Eaton, R. J.; Hursthouse, M. B.; Kılıç, A.; Shaw, R. A.; Uslu, A. *Eur. J. Org. Chem.* **2004**, 1881–1886.

(2) (a) Porwolik-Czomperlic, I.; Brandt, K.; Clayton, T. A.; Davies, D. B.; Eaton, R. J.; Shaw, R. A. *Inorg. Chem.* **2002**, *41*, 4944–4951. (b) Allcock, H. R.; Sunderland, N. J.; Primrose, A. P.; Rheingold, A. L.; Guzei, I. A.; Parvez, M. *Chem. Mater.* **1999**, *11*, 2478–2485. (c) Carriedo, G. A.; Martinez, J. I. F.; Alonso, F. J. G.; Gonzalez, E. R.; Soto, A. P. *Eur. J. Inorg. Chem.* **2002**, 1502–1510. (d) Chandrasekhar, V.; Athimoolam, A.; Srivatsan, S. G.; Sundaram, P. S.; Verma, S.; Steiner, A.; Zacchini, S.; Butcher, R. *Inorg. Chem.* **2002**, *41*, 5162–5173. (e) Bilge, S.; Demiriz, Ş.; Okumuş, A.; Kılıç, Z.; Tercan, B.; Hökelek, T.; Büyükgüngör, O. *Inorg. Chem.* **2006**, *45*, 8755–8767.

two Cl atoms in a cis nongeminal route to give ansa derivatives and in a geminal route to give spiro derivatives. In addition, only one of the two functional groups may react with $\text{N}_3\text{P}_3\text{Cl}_6$ to give open-chain (dangling) compounds, and the bifunctional reagents may replace two Cl atoms on two different phosphazene rings to form bridged (bino) phosphazene derivatives. On the other hand, intermolecular condensation reactions produce oligomers and cyclolinear or cyclomatrix polymers. In the formation of these phosphazene derivatives, many factors play an important role, e.g., solvent polarities, temperature, size of the phosphazene ring, and properties of the bifunctional ligands.^{1a,3} The stereogenic properties of cyclophosphazenes have highly attracted interest during the past decade.⁴ ^{31}P NMR spectroscopy upon the addition of a chiral solvating agent (CSA)^{4b,5} and high-performance liquid chromatography (HPLC) techniques⁶ have been very useful in the investigation of the stereogenic properties of phosphazenes.

Phosphazene derivatives are also of considerable interest in various areas such as advanced elastomers,⁷ rechargeable batteries,⁸ anticancer,⁹ antibacterial reagents,¹⁰ and biomedical materials.¹¹ The DNA binding abilities of phosphazenes are well-known¹² and can be examined by agarose gel electrophoresis.¹³

Recently, our group published the paper^{5c} about the antibacterial and antifungal activity of tetrapyrrolidinoferrocenylphosphazenes. So, pyrrolidino-substituted N/O spirocyclic phosphazenes are chosen in this study. As a particular interest in our ongoing studies about N/O spirocyclic phosphazene derivatives,¹⁴ we report here in detail (i) the preparation of new mono- (**2a**, **2b**, and **2e**), di- (**3a** and **3b**), and trispirocyclic (**4a** and **4b**) phosphazenes, (ii) the synthesis of tetra- (**2f–2i**) and dipyrrolidinophosphazenes (**3e–3h**), (iii) the preparation of *trans*-trispirocyclic derivatives (**3i–3k**) (Scheme 1), (iv) the stereogenic properties of **3a–3k**, which are investigated by ^{31}P NMR measurements in the presence of a CSA, (v) the determination of the structures of compounds by elemental analyses, mass spectrometry (MS), Fourier transform infrared (FTIR), one-dimensional (^1H , ^{13}C , and ^{31}P NMR, distortionless enhancement by polarization transfer (DEPT), and two-dimensional (2D) heteronuclear shift correlation (HETCOR), (vi) the solid-state structures of **2a**, **2e**, **2f**, **3e**, and **3f** established by X-ray diffraction techniques, (vii) investigations of the antibacterial and antifungal activity of **2f–2i**, **3e–3i**, and **3k**, and (xi) interactions between these compounds and pUC 18 plasmid DNA examined by agarose gel electrophoresis.

Experimental Section

General Methods. Reagents were of commercial grade and were used without further purification. Hexachlorocyclotriphosphazatriene was purchased from Aldrich. All experiments were carried out under an argon atmosphere. All reactions were monitored using thin-layer chromatography (TLC) in different solvents and chromatographed using silica gel. ^1H , ^{13}C , and ^{31}P NMR spectra were recorded on a Bruker DPX FT-NMR spectrometer (SiMe_4 as an internal standard and 85% H_3PO_4 as an external standard), operating at 499.94, 125.72, and 202.38 MHz. The spectrometer was equipped with a 5 mm PABBO BB inverse-gradient probe. Standard Bruker pulse programs were used. IR spectra were recorded on a Mattson 1000 FTIR spectrometer in KBr disks and were reported in reciprocal centimeter units. Microanalyses were carried out by the microanalytical service of TÜBİTAK-Turkey. MS spectra are recorded on a Bruker MicrOTOF LC-MS spectrometer using an electrospray ionization (ESI) method; ^{35}Cl values were used for calculated masses. Mycobacterial susceptibility testing was performed by the BACTEC MGIT 960 (Becton Dickinson, Sparks, MD) system (section S1 in the Supporting Information). The DNA binding abilities were examined using agarose gel electrophoresis (section S2 in the Supporting Information).

Preparation of Compounds. *N*-Benzyl- (**1a**),¹⁵ *N*-isopropyl- (**1b**),¹⁶ *N*-propyl- (**1c**),¹⁷ *N*-ethyl- (**1d**),¹⁷ and *N*-methyl-*o*-hydroxybenzylamine (**1e**)¹⁵ were synthesized according to the methods reported in the literature. Also, compounds **2c**, **2d**, **3c**, and **3d** were obtained from the reaction of **1c** and **1d** with $\text{N}_3\text{P}_3\text{Cl}_6$ according to the reported procedure.^{14a} The numbering of H and C atoms in phosphazene derivatives is given in Scheme 1.

4,4,6,6-Tetrachloro-3-benzyl-3,4-dihydrospiro[1.3.2]benzoxazaphosphorine[2 λ^5 ,4 λ^5 ,6 λ^5][1,3,5,2,4,6]triazatriphosphorine (2a**).** A solution of **1a** (2.00 g, 9.38 mmol) in tetrahydrofuran (THF; 50 mL) and triethylamine (2.17 mL) was slowly added to a stirred solution of $\text{N}_3\text{P}_3\text{Cl}_6$ (3.26 g, 9.38 mmol) in THF (100 mL)

(3) Allcock, H. R.; Diefenbach, U.; Pucher, S. R. *Inorg. Chem.* **1994**, *33*, 3091–3095.

(4) (a) İter, E. E.; Çaylak, N.; Işıklan, M.; Asmafiliz, N.; Kılıç, Z.; Hökelek, T. *J. Mol. Struct.* **2004**, *697*, 119–129. (b) Asmafiliz, N.; İter, E. E.; Işıklan, M.; Kılıç, Z.; Tercan, B.; Çaylak, N.; Hökelek, T.; Büyükgüngör, O. *J. Mol. Struct.* **2007**, *30*, 172–183. (c) Bhuvan Kumar, N. N.; Kumara Swamy, K. C. *Chirality* **2008**, *20*, 781–789.

(5) (a) Bešli, S.; Coles, S. J.; Davies, D. B.; Eaton, R. J.; Hursthouse, M. B.; Kılıç, A.; Shaw, R. A.; Uslu, A.; Yeşilot, Ş. *Inorg. Chem. Commun.* **2004**, *7*, 842–846. (b) Coles, S. J.; Davies, D. B.; Hursthouse, M. B.; Kılıç, A.; Şahin, Ş.; Shaw, R. A.; Uslu, A. *J. Organomet. Chem.* **2007**, *692*, 2811–2821. (c) Asmafiliz, N.; Kılıç, Z.; Öztürk, A.; Hökelek, T.; Koç, L. Y.; Açık, L.; Kısı, Ö.; Albay, A.; Üstündağ, Z.; Solak, A. O. *Inorg. Chem.* **2009**, *48*, 10102–10116.

(6) (a) Bui, T. T.; Coles, S. J.; Davies, D. B.; Drake, A. F.; Eaton, R. J.; Hursthouse, M. B.; Kılıç, A.; Shaw, R. A.; Yeşilot, Ş. *Chirality* **2005**, *17*, 438–443. (b) Bešli, S.; Davies, D. B.; Kılıç, A.; Shaw, R. A.; Şahin, Ş.; Uslu, A.; Yeşilot, Ş. *J. Chromatogr. A* **2006**, *1132*, 201–205. (c) Yeşilot, Ş.; Çoşut, B. *Inorg. Chem. Commun.* **2007**, *10*, 88–93. (d) Coles, S. J.; Davies, D. B.; Hursthouse, M. B.; Kılıç, A.; Çoşut, B.; Yeşilot, Ş. *Acta Crystallogr., Sect. B* **2009**, *65*, 355–362. (e) Çoşut, B.; İbişoğlu, H.; Kılıç, A.; Yeşilot, Ş. *Inorg. Chim. Acta* **2009**, *362*, 4931–4936.

(7) (a) Allcock, H. R.; Napierala, M. E.; Cameron, C. G.; O'Connor, S. J. M. *Macromolecules* **1996**, *29*, 1951–1956. (b) Allcock, H. R. *Curr. Opin. Solid State Mater. Sci.* **2006**, *10*, 231–240.

(8) (a) Xu, G.; Lu, Q.; Yu, B.; Wen, L. *Solid State Ionics* **2006**, *177*, 305–309. (b) Morford, R. V.; Kellam, E. C.; Hofmann, M. A.; Baldwin, R.; Allcock, H. R. *Solid State Ionics* **2000**, *133*, 171–177. (c) Allcock, H. R.; Kellam, E. C.; Morford, R. V.; Conner, D. A.; Welna, D. T.; Chang, Y.; Allcock, H. R. *Macromolecules* **2007**, *40*, 322–328. (d) Klein, R.; Welna, D. T.; Weikel, A.; Allcock, H. R.; Runt, J. *Macromolecules* **2007**, *40*, 3990–3995.

(9) (a) Porwolik-Czomperlik, I.; Siwy, M.; Şek, D.; Kaczmarczyk, B.; Nasulewicz, A.; Jaroszewicz, I.; Pelczynska, M.; Opolski, A. *Acta Polym. Pharm.* **2004**, *66*, 267–272. (b) Siwy, M.; Şek, D.; Kaczmarczyk, B.; Jaroszewicz, I.; Nasulewicz, A.; Pelczynska, M.; Nevozhay, D.; Opolski, A. *J. Med. Chem.* **2006**, *49*, 806–810.

(10) (a) Yılmaz, Ö.; Aslan, F.; Öztürk, A. İ.; Vanlı, N. S.; Kırbağ, S.; Arslan, M. *Bioorg. Chem.* **2002**, *30*, 303–314. (b) Konar, V.; Yılmaz, Ö.; Aslan, F.; Öztürk, A. İ.; Kırbağ, S.; Arslan, M. *Bioorg. Chem.* **2000**, *28*, 214–225.

(11) (a) Greish, Y. E.; Bender, J. D.; Lakshmi, S.; Brown, P. W.; Allcock, H. R.; Laurencin, C. T. *Biomaterials* **2005**, *26*, 1–9. (b) Nair, L.; Bhattacharyya, S.; Bender, J. D.; Greish, Y. E.; Brown, P. W.; Allcock, H.; Laurencin, C. T. *Biomacromolecules* **2004**, *5*, 2212–2220.

(12) (a) Grochowski, J.; Serda, P.; Brandt, K. *Drug Res. (Arzneim. Forsch.)* **1994**, *44*, 655–658. (b) Brandt, K.; Bartzak, T. J.; Kruszynski, R.; Porwolik-Czomperlik, I. *Inorg. Chim. Acta* **2001**, *322*, 138–144.

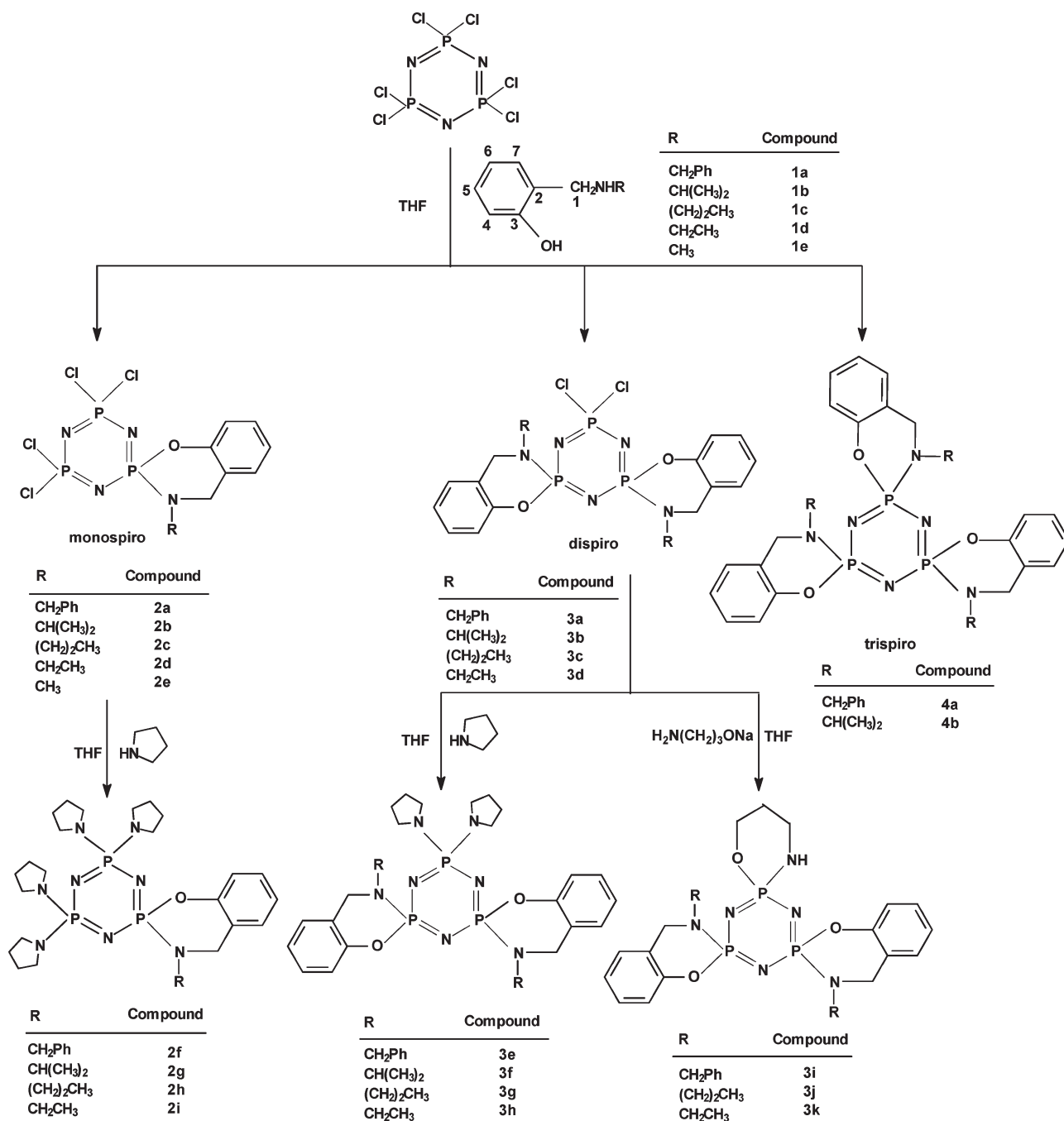
(13) Turner, P. C.; McLennan, A. G.; Bates, A. D.; White, M. R. H. *Molecular Biology*, 2nd ed.; Springer: Berlin, 2000.

(14) (a) İter, E. E.; Asmafiliz, N.; Kılıç, Z.; Işıklan, M.; Hökelek, T.; Çaylak, N.; Şahin, E. *Inorg. Chem.* **2007**, *46*, 9931–9944. (b) Işıklan, M.; Sonkaya, Ö.; Çoşut, B.; Yeşilot, Ş.; Hökelek, T. *Polyhedron* **2010**, *29*, 1612–1618.

(15) Andreu, R.; Ronda, J. C. *Synth. Commun.* **2008**, *38*, 2316–2329.

(16) Robertson, A.; Jones, D. G. Patent 681993, 1952.

(17) (a) Cromwell, N. H.; Hoeksema, H. *J. Am. Chem. Soc.* **1945**, *67*, 1658–1660. (b) Bar-Haim, G.; Kol, M. *Org. Lett.* **2004**, *6*(20), 3549–3551.

Scheme 1. Reaction Pathway of $N_3P_3Cl_6$ with *N*-Alkyl (or Aryl)-*o*-hydroxybenzylamines (**1a–1e**)

at room temperature. The mixture was stirred for 8 h, and the precipitated triethylamine hydrochloride was filtered off. The solvent was evaporated completely, and the oily residue was purified by column chromatography with toluene. The product was crystallized from *n*-hexane (ethyl acetate, $R_f = 0.85$). Yield: 4.00 g (87%). Mp: 96 °C. Anal. Calcd for $C_{14}H_{13}N_4OP_3Cl_4$: C, 34.46; H, 2.68; N, 11.48. Found: C, 34.57; H, 2.81; N, 11.42. ESI-MS (fragments were based on ^{35}Cl): m/z 487 $[M + H]^+$. FTIR (KBr, cm^{-1}): ν 3060, 3033 (C–H aromatic), 2916, 2862 (C–H aliphatic), 1248, 1179 (P=N), 572, 514 (P–Cl). 1H NMR ($CDCl_3$, ppm): δ 4.15 (d, 2H, $^3J_{PH} = 15.2$ Hz, H_1), 4.25 (d, 2H, $^3J_{PH} = 9.7$ Hz, NCH_2), 6.95–7.43 (9H, Ar–H). ^{13}C NMR ($CDCl_3$, ppm): δ 51.00 (d, $^2J_{PC} = 4.2$ Hz, NCH_2), 47.48 (C_1), 118.75 (d, $^3J_{PC} = 8.4$ Hz, C_4), 123.49 (d, $^3J_{PC} = 7.5$ Hz, C_2), 128.07 (C_7), 124.40 (C_6), 126.73, 128.35, 128.85 (Ar–C), 135.75 (d, $^3J_{PC} = 6.8$ Hz, Ar–C), 129.07 (C_5), 149.88 (d, $^2J_{PC} = 8.2$ Hz, C_3).

4,4,6,6-Tetrachloro-3-isopropyl-3,4-dihydrospiro[1.3.2]benzo-xazaphosphorine[2,5,4,5',6,5'']-[1,3,5,2,4,6]triazatriphosphorine (2b**).** The workup procedure was similar to that of compound **2a**, using **1b** (1.42 g, 8.61 mmol), $N_3P_3Cl_6$ (2.99 g, 8.61 mmol), and triethylamine (2.42 mL) (ethyl acetate, $R_f = 0.87$). Yield: 3.20 g (84%). Mp: 106 °C. Anal. Calcd for $C_{10}H_{13}N_4OP_3Cl_4$: C, 27.27; H, 2.95; N, 12.73. Found: C, 27.73; H, 2.72; N, 12.68. ESI-MS (fragments were based on ^{35}Cl): m/z 441 $[M + H]^+$. FTIR (KBr, cm^{-1}): ν 3072, 3034 (C–H aromatic), 2921, 2862 (C–H aliphatic), 1218, 1180 (P=N), 573, 515 (P–Cl). 1H NMR ($CDCl_3$, ppm): δ 1.28 [d, 6H, $^3J_{HH} = 6.5$ Hz, $CH(CH_3)_2$], 3.81 (m, 1H, $^3J_{HH} = 6.5$ Hz, $^3J_{PH} = 12.0$ Hz, NCH_2), 4.21 (d, 2H, $^3J_{PH} = 16.5$ Hz, H_1), 7.09–7.28 (4H, Ar–H). ^{13}C NMR ($CDCl_3$, ppm): δ 20.19 [d, $^2J_{PC} = 4.0$, $CH(CH_3)_2$], 41.22 (d, $^2J_{PC} = 2.5$ Hz, C_1), 47.23 [d, $^2J_{PC} = 5.0$ Hz, $CH(CH_3)_2$], 118.88 (d, $^3J_{PC} = 7.8$ Hz, C_4), 124.57 (C_6), 125.18 (d, $^3J_{PC} = 7.0$ Hz, C_2), 126.65 (C_5), 129.20 (C_7), 150.31 (d, $^2J_{PC} = 8.3$ Hz, C_3).

4,4,6,6-Tetrachloro-3-methyl-3,4-dihydrospiro[1.3.2]benzoxazaphosphorine[2 λ^5 ,4 λ^5 ,6 λ^5][1,3,5,2,4,6]triazatriphosphorine (**2e**). The workup procedure was similar to that of compound **2a**, using **1e** (1.39 g, 10.15 mmol), N₃P₃Cl₆ (3.53 g, 10.17 mmol), and triethylamine (2.85 mL). The oily residue was purified by column chromatography with benzene, and the product was crystallized from *n*-hexane (ethyl acetate, *R*_f = 0.86). Yield: 3.25 g (78%). Mp: 101 °C. Anal. Calcd for C₈H₉N₄OP₃Cl₄: C, 23.30; H, 2.18; N, 13.59. Found: C, 23.62; H, 2.15; N, 13.56. ESI-MS (fragments were based on ³⁵Cl): *m/z* 412 [M]⁺. FTIR (KBr, cm⁻¹): ν 3071, 3046 (C–H aromatic), 2959, 2859 (C–H aliphatic), 1261, 1163 (P=N), 577, 506 (P–Cl). ¹H NMR (CDCl₃, ppm): δ 2.80 (d, 3H, ³*J*_{PH} = 13.7 Hz, NCH₃), 4.28 (d, 2H, ³*J*_{PH} = 15.9 Hz, H₁), 7.05–7.35 (4H, Ar–H). ¹³C NMR (CDCl₃, ppm): δ 34.60 (d, ²*J*_{PC} = 2.7 Hz, NCH₃), 51.20 (C₁), 118.80 (d, ³*J*_{PC} = 8.7 Hz, C₄), 122.80 (d, ³*J*_{PC} = 7.3 Hz, C₂), 124.20 (C₆), 126.60 (C₅), 128.90 (C₇), 149.80 (d, ²*J*_{PC} = 7.9 Hz, C₃).

4,4,6,6-Pyrrolidino-3-benzyl-3,4-dihydrospiro[1.3.2]benzoxazaphosphorine[2 λ^5 ,4 λ^5 ,6 λ^5][1,3,5,2,4,6]triazatriphosphorine (**2f**). A solution of compound **2a** (1.20 g, 2.46 mmol) in dry THF (150 mL) was added slowly to a solution of pyrrolidine (2.42 mL, 29.53 mmol), and the resulting solution was then stirred and refluxed for 22 h. After excess triethylamine (1.72 mL) was added to the solution, the mixture was refluxed for another 3 h. The solvent was evaporated, and the oily product was purified by column chromatography using *n*-hexane–ethyl acetate (1:3) as an eluent. The product was crystallized from *n*-hexane (ethyl acetate, *R*_f = 0.69). Yield: 1.08 g (70%). Mp: 128 °C. Anal. Calcd for C₃₀H₄₅N₈OP₃: C, 57.50; H, 7.24; N, 17.88. Found: C, 57.16; H, 6.96; N, 17.77. ESI-MS (fragments were based on ³⁵Cl): *m/z* 627 [M + H]⁺. FTIR (KBr, cm⁻¹): ν 3060, 3033 (C–H aromatic), 2916, 2862 (C–H aliphatic), 1248, 1179 (P=N). ¹H NMR (CDCl₃, ppm): δ 1.83, 1.75 [m, 16H, NCH₂CH₂ (pyrr)], 3.21, 3.12 [d, 16H, ³*J*_{PH} = 10.0 Hz, NCH₂ (pyrr)], 4.11 (d, 2H, ³*J*_{PH} = 15.0 Hz, H₁), 4.26 (d, 2H, ³*J*_{PH} = 10.0 Hz, NCH₂), 6.90–7.48 (9H, Ar–H). ¹³C NMR (CDCl₃, ppm): δ 26.60, 26.63 [³*J*_{PC} = 8.8 Hz, NCH₂CH₂ (pyrr)], 46.43, 46.46 [²*J*_{PC} = 2.5 Hz, NCH₂ (pyrr)], 51.73 (d, ²*J*_{PC} = 2.5 Hz, NCH₂), 48.42 (C₁), 118.83 (d, ³*J*_{PC} = 7.5 Hz, C₄), 124.42 (d, ³*J*_{PC} = 7.5 Hz, C₂), 122.35 (C₆), 127.25 (C₅), 128.05 (C₇), 126.95, 128.51, 128.82 (Ar–C) 138.85 (d, ³*J*_{PC} = 8.8 Hz, Ar–C), 151.28 (d, ²*J*_{PC} = 7.5 Hz, C₃).

4,4,6,6-Pyrrolidino-3-isopropyl-3,4-dihydrospiro[1.3.2]benzoxazaphosphorine[2 λ^5 ,4 λ^5 ,6 λ^5][1,3,5,2,4,6]triazatriphosphorine (**2g**). The workup procedure was similar to that of compound **2f**, using **2b** (1.50 g, 3.54 mmol) and pyrrolidine (3.49 mL, 42.48 mmol). After excess triethylamine (2.46 mL) was added to the solution, the mixture was refluxed for another 4 h. The solvent was evaporated, and the crude product was purified by column chromatography with toluene–THF (3:1). The product was crystallized from acetonitrile (ethyl acetate, *R*_f = 0.55). Yield: 1.40 g (68%). Mp: 133 °C. Anal. Calcd for C₂₆H₄₅N₈OP₃: C, 53.98; H, 7.79; N, 19.38. Found: C, 54.75; H, 7.94; N, 18.91. ESI-MS (fragments were based on ³⁵Cl): *m/z* 579 [M + H]⁺. FTIR (KBr, cm⁻¹): ν 3078, 3044 (C–H aromatic), 2963, 2864 (C–H aliphatic), 1218, 1180 (P=N). ¹H NMR (CDCl₃, ppm): δ 1.12 [d, 3H, ³*J*_{HH} = 7.0 Hz, NCH(CH₃)₂], 1.18 [d, 3H, ³*J*_{HH} = 7.0 Hz, NCH(CH₃)₂], 1.76, 1.72 [m, 16H, ³*J*_{HH} = 6.6 Hz, NCH₂CH₂ (pyrr)], 3.08, 3.12 [m, 16H, ³*J*_{HH} = 6.6 Hz, NCH₂ (pyrr)], 3.92 (m, 1H, ³*J*_{HH} = 7.0 Hz, NCH), 4.10 (d, 2H, ³*J*_{PH} = 16.3 Hz, H₁), 6.83–7.09 (4H, Ar–H). ¹³C NMR (CDCl₃, ppm): δ 20.46 [d, ³*J*_{PC} = 4.3 Hz, CH(CH₃)₂], 26.51, 26.57 [³*J*_{PC} = 7.3 Hz, NCH₂CH₂ (pyrr)], 41.31 (d, ²*J*_{PC} = 6.7 Hz, C₁), 46.35 [d, ²*J*_{PC} = 7.5 Hz, CH(CH₃)₂], 46.26 [d, ²*J*_{PC} = 5.8 Hz, NCH₂ (pyrr)], 46.22 [d, ²*J*_{PC} = 5.7 Hz, NCH₂ (pyrr)], 118.61 (C₄), 122.26 (d, ³*J*_{PC} = 9.8 Hz, C₂), 127.81 (C₅), 126.46 (C₆), 127.89 (C₇), 152.15 (d, ²*J*_{PC} = 8.2 Hz, C₃).

4,4,6,6-Pyrrolidino-3-propyl-3,4-dihydrospiro[1.3.2]benzoxazaphosphorine[2 λ^5 ,4 λ^5 ,6 λ^5][1,3,5,2,4,6]triazatriphosphorine (**2h**). The workup procedure was similar to that of compound **2f**,

using **2c** (1.04 g, 2.36 mmol) and pyrrolidine (2.33 mL, 28.32 mmol). After excess triethylamine (1.66 mL) was added to the solution, the mixture was refluxed for another 4 h. The solvent was evaporated, and the crude product was purified by column chromatography with *n*-hexane–ethyl acetate (2:4) and crystallized from *n*-hexane (ethyl acetate, *R*_f = 0.63). Yield: 1.07 g (78%). Mp: 119 °C. Anal. Calcd for C₂₆H₄₅N₈OP₃: C, 53.97; H, 7.84; N, 19.37. Found: C, 53.87; H, 19.27; N, 7.71. ESI-MS (fragments were based on ³⁵Cl): *m/z* 579 [M]⁺. FTIR (KBr, cm⁻¹): ν 3057, 3039 (C–H aromatic), 2962, 2868 (C–H aliphatic), 1234, 1188 (P=N). ¹H NMR (CDCl₃, ppm): δ 0.87 (t, 3H, ³*J*_{HH} = 7.5 Hz, NCH₂CH₂CH₃), 1.63 (m, 2H, ³*J*_{HH} = 7.5 Hz, NCH₂CH₂), 1.72, 1.76 [m, 16H, ³*J*_{HH} = 6.3 Hz, NCH₂CH₂ (pyrr)], 2.99 (m, 2H, ³*J*_{HH} = 7.5 Hz, NCH₂), 3.08, 3.11 [m, 16H, ³*J*_{HH} = 6.3 Hz, NCH₂ (pyrr)], 4.21 (d, 2H, ³*J*_{PH} = 14.5 Hz, H₁), 6.82–7.09 (4H, Ar–H). ¹³C NMR (CDCl₃, ppm): δ 11.79 (NCH₂CH₂CH₃), 21.63 (d, ³*J*_{PC} = 5.0 Hz, NCH₂CH₂), 26.57 [dd, ³*J*_{PC} = 9.2 Hz, NCH₂CH₂ (pyrr)], 26.63 [dd, ³*J*_{PC} = 9.3 Hz, NCH₂CH₂ (pyrr)], 46.37, 46.25 [NCH₂ (pyrr)], 49.03 (C₁), 50.21 (d, ²*J*_{PC} = 2.3 Hz, NCH₂), 118.66 (d, ³*J*_{PC} = 7.5 Hz, C₄), 122.17 (C₆), 124.83 (d, ³*J*_{PC} = 7.5 Hz, C₂), 126.72 (C₅), 127.89 (C₇), 152.18 (d, ²*J*_{PC} = 7.9 Hz, C₃).

4,4,6,6-Pyrrolidino-3-ethyl-3,4-dihydrospiro[1.3.2]benzoxazaphosphorine[2 λ^5 ,4 λ^5 ,6 λ^5][1,3,5,2,4,6]triazatriphosphorine (**2i**). The workup procedure was similar to that of compound **2f**, using **2d** (1.44 g, 3.39 mmol) and pyrrolidine (3.33 mL, 40.56 mmol). After excess triethylamine (2.35 mL) was added to the solution, the mixture was refluxed for another 3 h. The solvent was evaporated, and the oily product was purified by column chromatography using *n*-hexane–ethyl acetate (1:4) as an eluent. The product was crystallized from *n*-hexane (ethyl acetate, *R*_f = 0.49). Yield: 1.52 g (79%). Mp: 106 °C. Anal. Calcd for C₂₅H₄₃N₈OP₃: C, 53.18; H, 7.68; N, 19.85. Found: C, 53.35; H, 7.58; N, 19.76. ESI-MS (fragments were based on ³⁵Cl): *m/z* 565 [M]⁺. FTIR (KBr, cm⁻¹): ν 3064, 3045 (C–H aromatic), 2961, 2865 (C–H aliphatic), 1240, 1197 (P=N). ¹H NMR (CDCl₃, ppm): 1.19 (t, 3H, ³*J*_{HH} = 7.0 Hz, NCH₂CH₃), 1.74, 1.77 [m, 16H, ³*J*_{HH} = 6.3 Hz, NCH₂CH₂ (pyrr)], 3.14 (m, 2H, ³*J*_{HH} = 7.0 Hz, NCH₂), 3.13, 3.17 [m, 16H, ³*J*_{HH} = 6.3 Hz, NCH₂ (pyrr)], 4.22 (d, 2H, ³*J*_{PH} = 14.5 Hz, H₁), 6.83–7.00 (4H, Ar–H). ¹³C NMR (CDCl₃, ppm): δ 13.66 (d, ³*J*_{PC} = 5.2 Hz, NCH₂CH₃), 26.64 [d, ³*J*_{PC} = 7.8 Hz, NCH₂CH₂ (pyrr)], 26.58 [d, ³*J*_{PC} = 8.0 Hz, NCH₂CH₂ (pyrr)], 42.63 (d, ²*J*_{PC} = 2.5 Hz, C₁), 48.32 (NCH₂), 46.27, 46.38 [NCH₂ (pyrr)], 118.65 (d, ³*J*_{PC} = 7.5 Hz, C₄), 122.23 (C₆), 124.83 (d, ³*J*_{PC} = 7.5 Hz, C₂), 126.77 (C₅), 127.90 (C₇), 152.10 (d, ²*J*_{PC} = 8.0 Hz, C₃).

6,6-Dichloro-trans-bis{3-benzyl-3,4-dihydrospiro[1.3.2]benzoxazaphosphorine}[2 λ^5 ,4 λ^5 ,6 λ^5][1,3,5,2,4,6]triazatriphosphorine (**3a**). A solution of compound **1a** (2.00 g, 9.38 mmol) in THF (100 mL) and triethylamine (5.27 mL) was slowly added to a stirred solution of N₃P₃Cl₆ (1.63 g, 4.69 mmol) in boiling THF (50 mL). The mixture was refluxed for 12 h, and the precipitated triethylamine hydrochloride was filtered off. The solvent was evaporated completely, and the oily residue was purified by column chromatography with benzene. The trans product was crystallized from *n*-heptane (ethyl acetate, *R*_f = 0.78). Yield: 1.98 g (67%). Mp: 113 °C. Anal. Calcd for C₂₈H₂₆N₅O₂P₃Cl₂: C, 53.55; H, 4.17; N, 11.15. Found: C, 53.67; H, 4.21; N, 11.42. ESI-MS (fragments were based on ³⁵Cl): *m/z* 628 [M + H]⁺. FTIR (KBr, cm⁻¹): ν 3060, 3031 (C–H aromatic), 2939, 2844 (C–H aliphatic), 1256, 1179 (P=N), 588, 510 (P–Cl). ¹H NMR (CDCl₃, ppm): δ 4.08–4.41 (4H, NCH₂), 4.08–4.41 (m, 4H, H₁), 6.95–7.50 (18H, Ar–H). ¹³C NMR (CDCl₃, ppm): δ 47.89 (C₁), 51.44 (d, ²*J*_{PC} = 2.5 Hz, NCH₂), 118.97 (C₄), 123.99 (C₂), 126.93 (C₅ and C₆), 127.97 (C₇), 128.91, 128.82, 136.91 (Ar–C), 150.58 (C₃).

6,6-Dichloro-trans-bis{3-isopropyl-3,4-dihydrospiro[1.3.2]benzoxazaphosphorine}[2 λ^5 ,4 λ^5 ,6 λ^5][1,3,5,2,4,6]triazatriphosphorine (**3b**). The workup procedure was similar to that of compound

3a, using **1b** (1.92 g, 11.64 mmol), $\text{N}_3\text{P}_3\text{Cl}_6$ (2.02 g, 5.82 mmol), and triethylamine (2.50 mL). The oily residue was purified by column chromatography with toluene. The trans product was crystallized from *n*-hexane (ethyl acetate, $R_f = 0.37$). Yield: 2.40 g (77%). Mp: 117 °C. Anal. Calcd for $\text{C}_{20}\text{H}_{26}\text{N}_5\text{O}_2\text{P}_3\text{Cl}_2$: C, 45.11; H, 4.89; N, 13.16. Found: C, 45.35; H, 4.98; N, 13.08. ESI-MS (fragments were based on ^{35}Cl): m/z 532 $[\text{M}]^+$. FTIR (KBr, cm^{-1}): ν 3064, 3048 (C–H aromatic), 2933, 2842 (C–H aliphatic), 1218, 1180 (P=N), 598, 510 (P–Cl). ^1H NMR (CDCl_3 , ppm): δ 1.30 (d, 6H, $^3J_{\text{HH}} = 6.5$ Hz, NCHCH_3), 1.35 (d, 6H, $^3J_{\text{HH}} = 6.5$ Hz, NCHCH_3), 4.00 (m, 1H, $^3J_{\text{HH}} = 6.5$ Hz, $^3J_{\text{PH}} = 12.3$ Hz, NCHCH_3), 4.29 (m, 1H, $^3J_{\text{HH}} = 6.5$ Hz, $^3J_{\text{PH}} = 13.5$ Hz, NCHCH_3), 4.15 (4H, $^2J_{\text{HH}} = 14.5$ Hz, $^3J_{\text{PH}} = 10.0$ Hz, H_1), 7.04–7.31 (8H, Ar–H). ^{13}C NMR (CDCl_3 , ppm): δ 20.18, 20.17 (NCHCH_3), 41.30 (C_1), 46.86 (NCHCH_3), 118.70 (t, $^3J_{\text{PC}} = 7.7$ Hz, C_4), 125.65 (d, $^3J_{\text{PC}} = 3.4$ Hz, C_2), 123.88 (C_6), 126.66 (C_5), 128.72 (C_7), 150.87 (d, $^2J_{\text{PC}} = 3.9$ Hz, C_3).

6,6-Pyrrolidino-trans-bis[3-benzyl-3,4-dihydrospiro[1.3.2]benzoxazaphosphorine][2 λ^5 ,4 λ^5 ,6 λ^5][1,3,5,2,4,6]triazatriphosphorine (3e). To a THF (75 mL) solution of **3a** (1.00 g, 1.59 mmol) was added 1.00 mL of pyrrolidine (12.70 mmol) in THF (75 mL), and the mixture was refluxed for 25 h. After excess triethylamine (0.89 mL) was added to the solution, the mixture was refluxed for another 4 h. The solvent was evaporated, and the crude product was purified by column chromatography with toluene–THF (7:1). The product was crystallized from *n*-hexane (ethyl acetate, $R_f = 0.45$). Yield: 0.60 g (54%). Mp: 142 °C. Anal. Calcd for $\text{C}_{36}\text{H}_{42}\text{N}_7\text{O}_2\text{P}_3$: C, 61.97; H, 6.07; N, 14.05. Found: C, 61.88; H, 6.02; N, 13.79. ESI-MS (fragments were based on ^{35}Cl): m/z 698 $[\text{M}]^+$. FTIR (KBr, cm^{-1}): ν 3062, 3028 (C–H aromatic), 2959, 2864 (C–H aliphatic), 1215, 1172 (P=N). ^1H NMR (CDCl_3 , ppm): δ 1.72, 1.79 [m, 8H, NCH_2CH_2 (pyrr)], 3.18 [m, 4H, $^3J_{\text{PH}} = 9.3$ Hz, NCH_2 (pyrr)], 3.30 [m, 4H, $^3J_{\text{PH}} = 9.2$ Hz, NCH_2 (pyrr)], 4.13 (2H, $^2J_{\text{HH}} = 14.8$ Hz, $^3J_{\text{PH}} = 7.6$ Hz, H_1), 4.16 (2H, $^2J_{\text{HH}} = 14.8$ Hz, $^3J_{\text{PH}} = 6.7$ Hz, H_1), 4.39 (4H, $^3J_{\text{PH}} = 9.8$ Hz, NCH_2), 7.15–7.55 (18H, Ar–H). ^{13}C NMR (CDCl_3 , ppm): δ 26.36 [d, $^3J_{\text{PC}} = 9.1$ Hz, NCH_2CH_2 (pyrr)], 51.51 (NCH_2), 46.10 [d, $^2J_{\text{PC}} = 4.0$ Hz, NCH_2 (pyrr)], 48.05 (C_1), 118.67 (dd, $^3J_{\text{PC}} = 7.9$ Hz, C_4), 122.65 (C_6), 124.31 (dd, $^3J_{\text{PC}} = 7.4$ Hz, C_2), 126.71 (C_5), 127.21 (C_7), 128.04, 128.40, 128.51 (Ar–C), 138.15 (d, $^3J_{\text{PC}} = 7.8$ Hz, Ar–C), 151.54 (dd, $^2J_{\text{PC}} = 7.5$ Hz, C_3).

6,6-Pyrrolidino-trans-bis[3-isopropyl-3,4-dihydrospiro[1.3.2]benzoxazaphosphorine][2 λ^5 ,4 λ^5 ,6 λ^5][1,3,5,2,4,6]triazatriphosphorine (3f). The workup procedure was similar to that of compound **3e**, using **3b** (0.90 g, 1.69 mmol) and pyrrolidine (1.11 mL, 13.52 mmol). After excess triethylamine (0.95 mL) was added to the solution, the mixture was refluxed for another 4 h (ethyl acetate, $R_f = 0.22$). Yield: 0.72 g (71%). Mp: 173 °C. Anal. Calcd for $\text{C}_{28}\text{H}_{42}\text{N}_7\text{O}_2\text{P}_3$: C, 55.91; H, 6.99; N, 16.31. Found: C, 55.96; H, 6.79; N, 16.22. ESI-MS (fragments were based on ^{35}Cl): m/z 602 $[\text{M}]^+$. FTIR (KBr, cm^{-1}): ν 3062, 3027 (C–H aromatic), 2964, 2865 (C–H aliphatic), 1242, 1178 (P=N). ^1H NMR (CDCl_3 , ppm): δ 1.22 (d, 6H, $^3J_{\text{HH}} = 7.5$ Hz, NCHCH_3), 1.24 (d, 6H, $^3J_{\text{HH}} = 7.5$ Hz, NCHCH_3), 1.81, 1.82 [m, 8H, NCH_2CH_2 (pyrr)], 3.15, 3.26 [m, 8H, NCH_2 (pyrr)], 4.02 (m, 2H, $^3J_{\text{HH}} = 7.5$ Hz, $^3J_{\text{PH}} = 11.0$ Hz, NCHCH_3), 4.14 (dd, 4H, $^2J_{\text{HH}} = 15.5$ Hz, $^3J_{\text{PH}} = 7.5$ Hz, H_1), 6.88–7.29 (8H, Ar–H). ^{13}C NMR (CDCl_3 , ppm): δ 20.12 (d, $^3J_{\text{PC}} = 3.2$ Hz, NCHCH_3), 20.64 (d, $^3J_{\text{PC}} = 5.5$ Hz, NCHCH_3), 26.66 [d, $^3J_{\text{PC}} = 9.1$ Hz, NCH_2CH_2 (pyrr)], 41.31 (C_1), 46.24 [d, $^2J_{\text{PC}} = 4.1$ Hz, NCH_2 (pyrr)], 46.26 (NCHCH_3), 118.55 (dd, $^3J_{\text{PC}} = 7.6$ Hz, C_4), 125.85 (dd, $^3J_{\text{PC}} = 6.7$ Hz, C_2), 122.65 (C_6), 126.60 (C_5), 128.00 (C_7), 151.86 (C_3).

6,6-Pyrrolidino-trans-bis[3-propyl-3,4-dihydrospiro[1.3.2]benzoxazaphosphorine][2 λ^5 ,4 λ^5 ,6 λ^5][1,3,5,2,4,6]triazatriphosphorine (3g). The workup procedure was similar to that of compound **3e**, using **3c** (0.90 g, 1.69 mmol) and pyrrolidine (1.11 mL, 13.52 mmol). After excess triethylamine (0.95 mL) was added to the solution, the mixture was refluxed for another 4 h. The

solvent was evaporated, and the product was purified by column chromatography using *n*-hexane–ethyl acetate (7:4) as an eluent (ethyl acetate, $R_f = 0.28$). Yield: 1.58 g (57%). Mp: 112 °C. Anal. Calcd for $\text{C}_{28}\text{H}_{42}\text{N}_7\text{O}_2\text{P}_3$: C, 55.90; H, 7.04; N, 16.29. Found: C, 56.19; H, 7.01; N, 16.13. ESI-MS (fragments were based on ^{35}Cl): m/z 602 $[\text{M}]^+$. FTIR (KBr, cm^{-1}): ν 3082, 3046 (C–H aromatic), 2959, 2870 (C–H aliphatic), 1224, 1167 (P=N). ^1H NMR (CDCl_3 , ppm): δ 0.95 (t, 6H, $^3J_{\text{HH}} = 7.4$ Hz, $\text{NCH}_2\text{CH}_2\text{CH}_3$), 1.70 (m, 4H, $^3J_{\text{HH}} = 7.4$ Hz, NCH_2CH_2), 1.82, 1.85 [m, 8H, NCH_2CH_2 (pyrr)], 3.09 (m, 4H, $^3J_{\text{PH}} = 13.1$ Hz, NCH_2), 3.15, 3.26 [m, 8H, NCH_2 (pyrr)], 4.22 (2H, $^2J_{\text{HH}} = 13.8$ Hz, $^3J_{\text{PH}} = 7.1$ Hz, H_1), 4.26 (2H, $^2J_{\text{HH}} = 14.6$ Hz, $^3J_{\text{PH}} = 7.7$ Hz, H_1), 6.90–7.17 (8H, Ar–H). ^{13}C NMR (CDCl_3 , ppm): δ 11.62 ($\text{NCH}_2\text{CH}_2\text{CH}_3$), 21.25 (d, $^3J_{\text{PC}} = 2.1$ Hz, NCH_2CH_2), 26.40 [d, $^3J_{\text{PC}} = 9.2$ Hz, NCH_2CH_2 (pyrr)], 46.00 [d, $^2J_{\text{PC}} = 4.1$ Hz, NCH_2 (pyrr)], 48.72 (NCH_2), 50.01 (C_1), 118.44 (dd, $^3J_{\text{PC}} = 7.8$ Hz, C_4), 122.38 (C_6), 124.64 (dd, $^3J_{\text{PC}} = 7.6$ Hz, C_2), 126.51 (C_5), 127.88 (C_7), 151.56 (dd, $^2J_{\text{PC}} = 7.7$ Hz, C_3).

6,6-Pyrrolidino-trans-bis[3-ethyl-3,4-dihydrospiro[1.3.2]benzoxazaphosphorine][2 λ^5 ,4 λ^5 ,6 λ^5][1,3,5,2,4,6]triazatriphosphorine (3h). The workup procedure was similar to that of compound **3g**, using **3d** (0.60 g, 1.69 mmol) and pyrrolidine (0.78 mL, 9.51 mmol). After excess triethylamine (0.49 mL) was added to the solution, the mixture was refluxed for another 3 h (ethyl acetate, $R_f = 0.69$). Yield: 1.53 g (55%). Mp: 134 °C. Anal. Calcd for $\text{C}_{26}\text{H}_{38}\text{N}_7\text{O}_2\text{P}_3$: C, 54.44; H, 6.67; N, 17.09. Found: C, 54.28; H, 6.34; N, 16.90. ESI-MS (fragments were based on ^{35}Cl): m/z 574 $[\text{M}]^+$. FTIR (KBr, cm^{-1}): ν 3071, 3045 (C–H aromatic), 2968, 2869 (C–H aliphatic), 1237, 1170 (P=N). ^1H NMR (CDCl_3 , ppm): δ 1.27 (t, 6H, $^3J_{\text{HH}} = 6.9$ Hz, NCH_2CH_3), 1.80, 1.84 [m, 8H, NCH_2CH_2 (pyrr)], 3.18 (m, 4H, $^3J_{\text{HH}} = 6.9$ Hz, NCH_2), 3.21, 3.25 [m, 8H, NCH_2 (pyrr)], 4.21 (2H, $^2J_{\text{HH}} = 14.7$ Hz, $^3J_{\text{PH}} = 7.8$ Hz, H_1), 4.24 (2H, $^2J_{\text{HH}} = 14.5$ Hz, $^3J_{\text{PH}} = 8.1$ Hz, H_1), 6.90–7.17 (8H, Ar–H). ^{13}C NMR (CDCl_3 , ppm): δ 13.24 (NCH_2CH_3), 26.37 [d, $^3J_{\text{PC}} = 9.1$ Hz, NCH_2CH_2 (pyrr)], 42.51 (NCH_2), 46.01 [d, $^2J_{\text{PC}} = 3.8$ Hz, NCH_2 (pyrr)], 48.03 (C_1), 118.43 (C_4), 122.37 (C_5), 124.52 (dd, $^3J_{\text{PC}} = 7.1$ Hz, C_2), 126.52 (C_6), 127.81 (C_7), 151.00 (dd, $^2J_{\text{PC}} = 8.0$ Hz, C_3).

Spiro(propene-3-amino-1-oxy)-trans-bis[3-benzyl-3,4-dihydrospiro[1.3.2]benzoxazaphosphorine][2 λ^5 ,4 λ^5 ,6 λ^5][1,3,5,2,4,6]triazatriphosphorine (3i). To a THF (150 mL) solution of **3a** (1.00 g, 1.59 mmol) were added sodium 3-amino-1-propanoxide (0.15 g, 1.59 mmol) and triethylamine (0.89 mL) at room temperature. The mixture was refluxed for 26 h, and the precipitated triethylamine hydrochloride and sodium chloride were filtered off. After the solvent was evaporated completely, the oily residue was purified by column chromatography using toluene–THF (2:1) as an eluent (ethyl acetate, $R_f = 0.31$). Yield: 0.53 g (53%). Mp: 177–179 °C. Anal. Calcd for $\text{C}_{31}\text{H}_{33}\text{N}_6\text{O}_3\text{P}_3$: C, 59.05; H, 5.27; N, 13.33. Found: C, 59.09; H, 5.32; N, 12.90. ESI-MS (fragments were based on ^{35}Cl): m/z 631 $[\text{M}]^+$. FTIR (KBr, cm^{-1}): ν 3364 (N–H), 3060, 3026 (C–H aromatic), 2932, 2851 (C–H aliphatic), 1239, 1184 (P=N). ^1H NMR (CDCl_3 , ppm): δ 1.85 (m, 2H, OCH_2CH_2), 2.58 (bp, 1H, NH), 3.38 (m, 2H, NHCH_2), 4.11–4.43 (4H, NCH_2), 4.11–4.43 (m, 4H, H_1), 4.11–4.43 (m, 2H, OCH_2), 6.92–7.53 (18H, Ar–H). ^{13}C NMR (CDCl_3 , ppm): δ 26.46 (d, $^3J_{\text{PC}} = 6.2$ Hz, OCH_2CH_2), 41.47 (d, $^2J_{\text{PC}} = 3.5$ Hz, NHCH_2), 48.44, 48.07 (C_1), 51.36, 51.79 (d, $^2J_{\text{PC}} = 3.4$ Hz, NCH_2), 67.46 (d, $^2J_{\text{PC}} = 6.8$ Hz, OCH_2), 118.91 (d, $^3J_{\text{PC}} = 7.3$ Hz, C_4), 119.07 (d, $^3J_{\text{PC}} = 6.9$ Hz, C_4), 123.21, 123.18 (C_6), 123.98 (d, $^3J_{\text{PC}} = 7.3$ Hz, C_2), 124.18 (d, $^3J_{\text{PC}} = 7.2$ Hz, C_2), 126.81, 126.97 (C_5), 128.79, 128.90 (C_7), 127.54, 127.57, 128.67, 128.71, 137.83, 137.89, 138.01, 138.06 (Ar–C), 151.22 (dd, $^2J_{\text{PC}} = 6.7$ Hz, C_3).

Spiro(propene-3-amino-1-oxy)-trans-bis[3-propyl-3,4-dihydrospiro[1.3.2]benzoxazaphosphorine][2 λ^5 ,4 λ^5 ,6 λ^5][1,3,5,2,4,6]triazatriphosphorine (3j). The workup procedure was similar to that of compound **3i**, using **3c** (1.20 g, 2.26 mmol), sodium 3-amino-1-propanoxide (0.22 g, 2.26 mmol), and triethylamine (0.64 mL)

Table 1. Crystallographic Details

	2a	2e	2f	3e	3f
empirical formula	C ₁₄ H ₁₃ Cl ₄ N ₄ O ₃ P ₃	C ₈ H ₉ Cl ₄ N ₄ O ₃ P ₃	C ₃₀ H ₄₅ N ₈ O ₃ P ₃	C ₃₆ H ₄₂ N ₇ O ₂ P ₃	C ₂₈ H ₄₂ N ₇ O ₂ P ₃
fw	487.99	411.90	626.65	697.68	601.60
cryst syst	orthorhombic	triclinic	monoclinic	monoclinic	triclinic
space group	<i>Pbcn</i>	<i>P</i> $\bar{1}$	<i>C2/c</i>	<i>P2₁/c</i>	<i>P</i> $\bar{1}$
<i>a</i> (Å)	27.1183(5)	8.5545(4)	23.8685(4)	10.8726(2)	8.498(2)
<i>b</i> (Å)	7.8779(2)	12.1377(3)	9.2096(1)	26.8581(4)	10.475(3)
<i>c</i> (Å)	19.4131(3)	16.6964(4)	28.8084(4)	12.8439(2)	17.969(4)
α (deg)	90	84.618(3)	90	90	80.235(4)
β (deg)	90	77.680(4)	92.884(1)	111.767(1)	79.155(3)
γ (deg)	90	74.287(5)	90	90	72.103(3)
<i>V</i> (Å ³)	4147.32(15)	1629.21(11)	6324.62(15)	3483.22(10)	1484.2(6)
<i>Z</i>	8	4	8	4	2
μ (cm ⁻¹)	0.814 (Mo K α)	1.019 (Mo K α)	0.227 (Mo K α)	0.215 (Mo K α)	0.240 (Mo K α)
ρ_{calcd} (g cm ⁻³)	1.563	1.679	1.316	1.330	1.346
no. of total reflns	4185	6603	5573	6131	5229
no. of unique reflns	4186	7065	39 818	24 664	23 857
<i>R</i> _{int}	0.0025	0.0424	0.0249	0.0263	0.0210
2 θ_{max} (deg)	52.60	52.58	50.04	50.06	50.06
<i>T</i> _{min} / <i>T</i> _{max}	0.780/0.812	0.780/0.855	0.9413/0.9582	0.9482/0.9623	0.9229/0.9403
no. of param	257	364	379	433	365
<i>R</i> [<i>F</i> ² > 2 σ (<i>F</i> ²)]	0.0549	0.0749	0.0402	0.0399	0.0342
<i>wR</i>	0.1330	0.1840	0.1089	0.1039	0.0892

(ethyl acetate, *R*_f = 0.25). Yield: 0.61 g (51%). Mp: 127 °C. Anal. Calcd for C₂₃H₃₃N₆O₃P₃: C, 51.68; H, 6.22; N, 15.72. Found: C, 51.32; H, 5.93; N, 15.58. ESI-MS (fragments were based on ³⁵Cl): *m/z* 535 [M + H]⁺. FTIR (KBr, cm⁻¹): ν 3274 (N–H), 3065, 3044 (C–H aromatic), 2959, 2871 (C–H aliphatic), 1235, 1168 (P=N). ¹H NMR (CDCl₃, ppm): δ 0.96 (t, 6H, ³*J*_{HH} = 6.9 Hz, NCH₂CH₂CH₃), 1.70 (m, 4H, ³*J*_{HH} = 6.9 Hz, NCH₂CH₂), 1.82 (m, 2H, OCH₂CH₂), 2.60 (bp, 1H, *NH*), 3.07 (m, 4H, NCH₂), 3.40 (m, 2H, NHCH₂), 4.22, 4.31 (m, 4H, H₁), 4.42 (m, 2H, OCH₂), 6.93–7.17 (8H, Ar–H). ¹³C NMR (CDCl₃, ppm): δ 11.57, 11.63 (NCH₂CH₂CH₃), 21.14 (d, ³*J*_{PC} = 11.6 Hz, OCH₂CH₂), 26.24 (d, ³*J*_{PC} = 6.6 Hz, NCH₂CH₂), 48.55 (NCH₂), 49.65, 49.77 (C₁), 41.20 (NHCH₂), 67.00 (d, ²*J*_{PC} = 6.8 Hz, OCH₂), 118.59 (dd, ³*J*_{PC} = 7.2 Hz, C₄), 118.67 (dd, ³*J*_{PC} = 8.0 Hz, C₄), 122.70, 122.75 (C₆), 124.24 (dd, ³*J*_{PC} = 6.3 Hz, C₂), 126.40, 126.52 (C₅), 127.98, 128.02 (C₇), 151.14 (C₃).

Spiro(propane-3-amino-1-oxy)-trans-bis[3-ethyl-3,4-dihydrospiro[1.3.2]benzoxazaphosphorine][2 λ^5 ,4 λ^5 ,6 λ^5][1,3,5,2,4,6]triazatriphosphorine (3k). The workup procedure was similar to that of compound 3i, using 3d (0.85 g, 1.68 mmol), sodium 3-amino-1-propanoxide (0.16 g, 1.68 mmol), and triethylamine (0.94 mL) (ethyl acetate, *R*_f = 0.28). Yield: 0.45 g (53%). Mp: 124 °C. Anal. Calcd for C₂₁H₂₉N₆O₃P₃: C, 49.81; H, 5.77; N, 16.60. Found: C, 49.71; H, 5.56; N, 16.38. ESI-MS (fragments were based on ³⁵Cl): *m/z* 507 [M + H]⁺. FTIR (KBr, cm⁻¹): ν 3264 (N–H), 3065, 3044 (C–H aromatic), 2968, 2871 (C–H aliphatic), 1240, 1177 (P=N). ¹H NMR (CDCl₃, ppm): δ 1.23 (d, 3H, ³*J*_{HH} = 7.0 Hz, NCH₂CH₃), 1.25 (d, 3H, ³*J*_{HH} = 7.0 Hz, NCH₂CH₃), 1.77 (m, 2H, OCH₂CH₂), 2.65 (bp, 1H, *NH*), 3.18 (m, 4H, ³*J*_{HH} = 7.0 Hz, NCH₂), 3.36 (m, 2H, NHCH₂), 4.17, 4.22 (m, 4H, H₁), 4.40 (m, 2H, OCH₂), 6.92–7.15 (8H, Ar–H). ¹³C NMR (CDCl₃, ppm): δ 13.27 (d, ³*J*_{PC} = 6.7 Hz, NCH₂CH₃), 13.42 (d, ³*J*_{PC} = 6.3 Hz, NCH₂CH₃), 26.49 (d, ³*J*_{PC} = 6.3 Hz, OCH₂CH₂), 41.41 (d, ²*J*_{PC} = 3.6 Hz, NHCH₂), 42.58, 42.65 (NCH₂), 48.08, 48.14 (C₁), 67.32 (d, ²*J*_{PC} = 6.8 Hz, OCH₂), 118.71, 118.87 (d, ³*J*_{PC} = 4.2 Hz, C₄), 123.02, 123.06 (C₆), 124.39 (d, ³*J*_{PC} = 3.5 Hz, C₂), 126.82, 126.72 (C₅), 128.24, 128.26 (C₇), 151.25 (dd, ²*J*_{PC} = 6.9 Hz, C₃).

Tris[3-benzyl-3,4-dihydrospiro[1.3.2]benzoxazaphosphorine]-[2 λ^5 ,4 λ^5 ,6 λ^5][1,3,5,2,4,6]triazatriphosphorine (4a). A solution of 1a (2.30 g, 10.80 mmol) in THF (100 mL) and triethylamine (4.55 mL) was slowly added to a stirred solution of N₃P₃Cl₆ (1.25 g, 3.60 mmol) in boiling THF (50 mL). The mixture was refluxed for 21 h, and the precipitated triethylamine hydrochloride was filtered off. The solvent was evaporated completely, and the oily residue was purified by column chromatography

with benzene. The product was crystallized from *n*-heptane (ethyl acetate, *R*_f = 0.52). Yield: 0.77 g (28%). Mp: 67 °C. Anal. Calcd for C₄₂H₃₉N₆O₃P₃: C, 65.62; H, 5.08; N, 10.94. Found: C, 65.56; H, 5.18; N, 10.76. ESI-MS (fragments were based on ³⁵Cl): *m/z* 769 [M]⁺. FTIR (KBr, cm⁻¹): ν 3060, 3043 (C–H aromatic), 2896, 2846 (C–H aliphatic), 1240, 1172 (P=N). ¹H NMR (CDCl₃, ppm): δ 4.09–4.45 (m, 6H, NCH₂), 4.09–4.45 (m, 6H, H₁), 6.96–7.41 (27H, Ar–H). ¹³C NMR (CDCl₃, ppm): δ 48.07 (C₁), 51.40 (NCH₂), 119.12, 123.27, 124.62, 126.90, 128.69, 127.55, 127.61 (Ar–C), 150.00 (C₃).

X-ray Crystal Structure Determinations. The colorless crystals of compounds 2a, 2e, 2f, 3e, and 3f were crystallized by the slow evaporation of solutions of the compounds in *n*-hexane at room temperature. The crystallographic data are given in Table 1, selected bond lengths and angles are listed in Table 2, and hydrogen-bond data are given in Table 3. Crystallographic data for compounds 2a and 2e were recorded on an Enraf-Nonius CAD-4 diffractometer using Mo K α radiation (λ = 0.710 73 Å) at *T* = 294(2) K, and absorption corrections by ψ scan¹⁸ were applied. Crystallographic data for compounds 2f, 3e, and 3f were recorded on a Bruker Kappa APEXII CCD area-detector diffractometer using Mo K α radiation (λ = 0.71073 Å) at *T* = 150(2) K (for 2f and 3e) and at *T* = 120(2) K (for 3f), and absorption corrections by multiscan^{19a} were applied. Structures were solved by direct methods and refined by full-matrix least squares against *F*² using all data.^{19b} All non-H atoms were refined anisotropically. H-atom positions were calculated geometrically at distances of 0.93 (CH), 0.97 (CH₂), and 0.96 (CH₃) Å (for compounds 2a and 2e) and at distances of 0.95 (aromatic CH), 1.00 (methine CH), 0.99 (CH₂), and 0.98 (CH₃) (for compounds 2f, 3e, and 3f) from the parent C atoms; a riding model was used during the refinement process, and the *U*_{iso}(H) values were constrained to be 1.5*U*_{eq}(carrier atom) (for CH₃) and 1.2*U*_{eq}(carrier atom) (for all other H atoms). In compound 2a, Cl atoms attached at P2 are disordered over two orientations. During the refinement process, the disordered Cl1, Cl2, Cl1', and Cl2' atoms were refined with occupancies of 0.60(3), 0.65(3), 0.40(3), and 0.35(3), respectively.

Results and Discussion

Synthesis. The spirocyclic phosphazene derivatives (2a–2i, 3a–3k, 4a, and 4b) have been synthesized from

(18) North, A. C. T.; Phillips, D. C.; Mathews, F. S. *Acta Crystallogr., Sect. A* **1968**, *24*, 351–359.

(19) (a) *SADABS*; Bruker AXS Inc.: Madison, WI, 2005. (b) Sheldrick, G. M. *Acta Crystallogr., Sect. A* **2008**, *64*, 112–122.

Table 2. Selected Bond Lengths (Å) and Angles (deg) for **2a**, **2e**, **2f**, **3e**, and **3f**

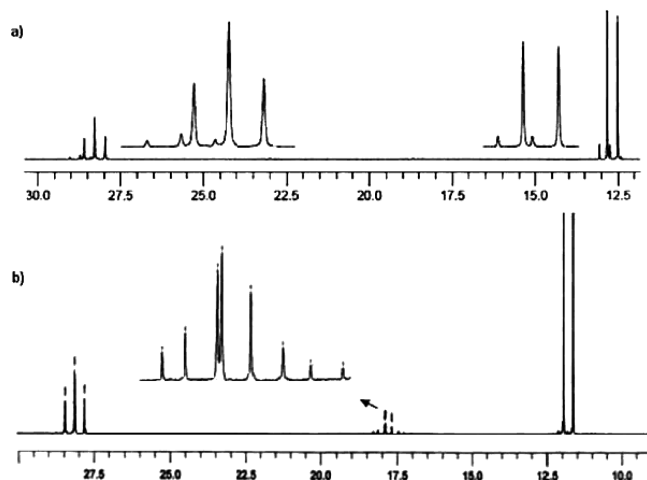
	2a	2e	2e'	2f	3e	3f
P1–N1	1.596(3)	1.588(4)	1.596(4)	1.583(2)	1.579(2)	1.593(2)
P1–N3	1.591(3)	1.587(3)	1.596(3)	1.575(2)	1.580(2)	1.571(2)
P1–N4	1.613(3)	1.617(3)	1.627(3)	1.662(2)	1.663(2)	1.649(1)
P1–O1	1.580(3)	1.572(3)	1.567(3)	1.626(1)	1.612(2)	1.618(1)
P2–N1	1.553(3)	1.555(4)	1.550(4)	1.606(2)	1.596(2)	1.588(1)
P2–N2	1.575(4)	1.565(4)	1.570(4)	1.591(2)	1.577(2)	1.591(1)
P2–N5					1.648(2)	1.642(1)
P2–O2					1.610(1)	1.616(1)
P3–N2	1.561(4)	1.568(4)	1.571(4)	1.596(2)	1.602(2)	1.605(1)
P3–N3	1.548(3)	1.556(3)	1.557(3)	1.610(2)	1.601(2)	1.607(1)
N1–P1–N3	113.7(2)	113.8(2)	113.2(2)	119.1(1)	117.8(1)	116.7(1)
N1–P2–N2	119.9(2)	119.5(2)	119.9(2)	115.7(1)	116.4(1)	116.6(1)
N5–P2–N6				100.9(1)		
N5–P2–O2					101.4(1)	101.3(1)
N7–P3–N8				101.4(1)		
N6–P3–N7					102.0(1)	101.6(1)
N2–P3–N3	119.8(2)	119.4(2)	119.8(2)	115.3(1)	114.6(1)	114.3(1)
N4–P1–O1	103.7(2)	103.6(2)	103.6(2)	103.3(1)	100.5(1)	101.3(1)
P1–N1–P2	122.5(2)	123.9(2)	118.7(2)	120.9(1)	122.1(1)	120.0(1)
P2–N2–P3	118.4(2)	119.3(2)	123.9(2)	124.3(1)	124.3(1)	121.8(1)
P1–N3–P3	124.1(2)	123.9(2)	127.2(2)	121.6(1)	123.2(1)	120.9(1)

Table 3. Hydrogen-Bond Geometries (Å, deg) for **2a**, **2f**, **3e**, and **3f**^a

	D–H···A	D–H	H···A	D···A	D–H···A
2a	C8–H8A···N3	0.97	2.74	3.107(6)	103
	C10–H10···N3	0.93	2.69	3.469(6)	142
2f	C8–H8A···N3	0.99	2.42	2.969(3)	114
	C2–H2···O1 ⁱ	0.95	2.64	3.282(3)	125
	C21–H21A···N2 ⁱⁱ	0.99	2.57	3.551(3)	171
3e	C8–H8B···N1	0.99	2.71	3.174(3)	109
	C19–H19···N1 ⁱⁱⁱ	0.95	2.69	3.456(3)	138
3f	C8–H8···N3	1.00	2.65	3.160(2)	111

^a Symmetry codes: (i) $-x, y, 1/2 - z$; (ii) $-x, -y, -z$, (iii) $x, 1/2 - y, 1/2 + z$.

the reactions of N/O-donor-type *N*-alkyl (or aryl)-*o*-hydroxybenzylamines (**1a–1e**) with $\text{N}_3\text{P}_3\text{Cl}_6$ in dry THF. All of the reactions of $\text{N}_3\text{P}_3\text{Cl}_6$ with the N/O bifunctional ligands (**1a–1e**) appear to be regioselective because only the spirocyclic derivatives have formed (Scheme 1). The reactions of equal amounts of $\text{N}_3\text{P}_3\text{Cl}_6$ and **1a–1e** in THF with triethylamine as an HCl acceptor afford corresponding monospirocyclic phosphazenes (**2a–2e**) at ambient temperature. The tetrapyrrolidino-phosphazenes (**2f–2i**) have been obtained from the reactions of **2a–2d** with excess pyrrolidine. When the reactions have been carried out with 1 equiv of $\text{N}_3\text{P}_3\text{Cl}_6$ and 2 equiv of **1a–1d**, corresponding dispirocyclic phosphazenes (**3a–3d**) are isolated. The ^{31}P NMR spectra of reaction mixtures of **3a–3d** indicate that cis and trans geometric isomers are present (Figure 1a). Only the trans isomers are separated by column chromatography. The bispyrrolidino dispirocyclic phosphazenes (**3e–3h**) are prepared by the reactions of **3a–3d** with excess pyrrolidine. The 3-amino-1-propanoxy derivatives (**3i–3k**), which are the trispirocyclic compounds, are obtained from the reactions of dispirocyclic phosphazenes (**3a**, **3c**, and **3d**) with sodium 3-amino-1-propanoxide. In addition, $\text{N}_3\text{P}_3\text{Cl}_6$ with excess **1a** and **1b** gives trispirocyclic phosphazenes **4a** and **4b**, respectively. Figure 1b indicates that the yield of **4b** is very low; thus, it could not have been isolated from the reaction mixture. The yields are variable depending on mono-, di-, and trisubstitutions of the phosphazene derivatives. All of the new phosphazenes are purified by column chromatography, except the cis isomers. In addition, *N*-benzyl (**4a**) and *N*-isopropyl-substituted (**4b**) trispirocyclic phosphazenes are expected to exist as cis–trans–trans or cis–cis–cis geometric isomers. Both of them are found to be in cis–trans–trans forms according to the ^{31}P NMR spectra of **4a** and **4b** (Figure 1b for **4b**). Similar structures are observed for the analogous compounds *N*-propyl- and *N*-ethyl-substituted trispirocyclic phosphazenes.^{14a}

**Figure 1.** ^1H -decoupled ^{31}P NMR spectra of reaction mixtures of (a) **3d** and (b) **4b**.

zemes are purified by column chromatography, except the cis isomers. In addition, *N*-benzyl (**4a**) and *N*-isopropyl-substituted (**4b**) trispirocyclic phosphazenes are expected to exist as cis–trans–trans or cis–cis–cis geometric isomers. Both of them are found to be in cis–trans–trans forms according to the ^{31}P NMR spectra of **4a** and **4b** (Figure 1b for **4b**). Similar structures are observed for the analogous compounds *N*-propyl- and *N*-ethyl-substituted trispirocyclic phosphazenes.^{14a}

NMR and IR Spectroscopy. The ^1H -decoupled ^{31}P NMR spectral data of all of the compounds indicate that they have spirocyclic derivatives. The spin systems are interpreted as simple AB_2 , AX_2 , A_2B , and A_2X , while the different substitution patterns at the P atoms of all of the compounds (Table 4) give rise to one triplet and one doublet in the ^1H -decoupled ^{31}P NMR spectra, except **4a** and **4b**. The spectra of **4a** and **4b** exhibit a total of eight signals for AB_2 spin systems ($^2J_{\text{PP}}/\Delta\nu = 1.4$ for **4a** and 0.5 for **4b**).²⁰ These results are unambiguously in agreement with the two kinds of P atoms present in the cyclophosphazene ring.

The dispirophosphazenes (**3a–3h**) having two equivalent stereogenic P atoms are expected to exist as cis and trans geometric isomers, which are considered as meso and racemic forms, respectively. In addition, the trispirocyclic derivatives (**3i–3k**) have three stereogenic P atoms. In order to predict the stereogenic properties of the trispirocyclic derivatives (**3i–3k**), the two equivalent chiral centers $\text{P}(\text{OArN})$ are labeled as *R/S* and the other stereogenic centers are labeled as *R'/S'*. Hence, the theoretical stereoisomeric distribution and expected geometrical isomers are summarized in Table 5. According to these analyses, compounds **3i–3k** have a racemate (trans) and two meso (cis) forms. However, the only racemic (trans) mixtures are obtained because the starting compounds **3a**, **3c**, and **3d** are racemic (trans).

As was mentioned before, the ^{31}P NMR spectra of reaction mixtures of **3a–3d** indicate that cis and trans geometric isomers are present. As an example, the ^1H -decoupled ^{31}P NMR spectrum of the reaction mixture of compound **3d** is depicted in Figure 1a. The cis and trans

Table 4. ^{31}P NMR (Decoupled) Spectral Data of the Compounds (δ Reported in ppm and J Values in Hz)^a

X = Cl or pyr

compound	spin system	δ (ppm)				$^2J_{\text{PP}}$ (Hz)
		PCl_2	P(OArN)	P(pyr)_2	P(ORN)	
2a	AX_2	24.22	5.86			56.6
2b	AX_2	24.71	5.44			56.2
2e	AX_2	25.41	7.67			55.9
2f	AB_2		19.04	20.31		50.1
2g	AX_2		17.66	20.31		48.6
2h	AB_2		18.60	20.27		48.5
2i	AB_2		18.39	20.33		46.5
3a (trans)	A_2X	29.07	13.15			64.4
3a (cis)	A_2X	33.50	14.15			62.0
3b (trans)	A_2X	28.20	11.70			65.3
3b (cis)	A_2X	28.37	11.82			63.7
3c (trans)^b	A_2B	28.60	12.70			64.5
3c (cis)	A_2X	28.71	12.91			62.8
3d (trans)^b	A_2B	28.60	12.30			63.8
3d (cis)	A_2X	28.91	12.50			62.5
3e	A_2B		18.67	21.74 (t)		53.1
3f	A_2X		17.37	21.67 (t)		53.3
3g	A_2X		18.21	21.61 (t)		52.5
3h	A_2X		18.14	21.78 (t)		52.1
3i	A_2B		17.55		20.10	63.5
3j	A_2B		17.43		19.93	63.3
3k	A_2X		16.97		20.12	62.4
4a	AB_2		17.88			50.7
4b	AB_2		18.38			45.1
			17.57			
4b	AB_2		17.92			

^a ^{31}P NMR measurements in CDCl_3 solutions at 293 K. ^b The ^{31}P NMR data of **3c** (trans) and **3d** (trans) are taken from ref 14a.

Table 5. Theoretical Stereoisomer Distribution and the Expected Geometrical Isomers of Compounds **3a–3h** and **3i–3k**

compounds	stereogenic P atoms (n)	stereoisomers ^a (2^n)		chirality	geometrical isomers
3a–3h	2	1	RR	racemic (lines 1/4)	trans
		2	RS	meso (lines 2 = 3)	cis
		3	SR		
		4	SS		
3i–3k	3	1	RRR'	racemic (lines 1/8 = 4/5)	trans
		2	RSR'		
		3	SRR'	meso ₁ (lines 2 = 7)	cis
		4	SSR'		
		5	RRS'	meso ₂ (lines 3 = 6)	cis
		6	RSS'		
		7	SRS'		
		8	SSS'		

^a Spiro-substituted groups P(OArN) labeled as R/S and P(ORN) labeled as R'/S' .

geometric isomers of **3d** are separated by preparative TLC (Figure 2). It is observed that the trans isomer of **3d**^{14a} yields approximately 90% and the cis isomer yields ca. 10%. The δ and J values of the cis isomers for **3a–3c** are calculated from ^{31}P NMR spectra of reaction mixtures (Table 4). These results are explained in terms of the cyclophosphazene chemistry, where trans derivatives predominate over their cis isomers because of steric effects

(Figure 3a).²¹ Moreover, in **3e–3k**, the trans isomers are obtained because only the trans isomers of **3a–3d** reacted with pyrrolidine and sodium 3-amino-1-propanoxide (Scheme 1). In addition, trans structures of **3e** and **3f** have been verified by the crystallographic results (see the crystallographic part).

(21) Allen, C. W. *Chem. Rev.* **1991**, *91*, 119–135.

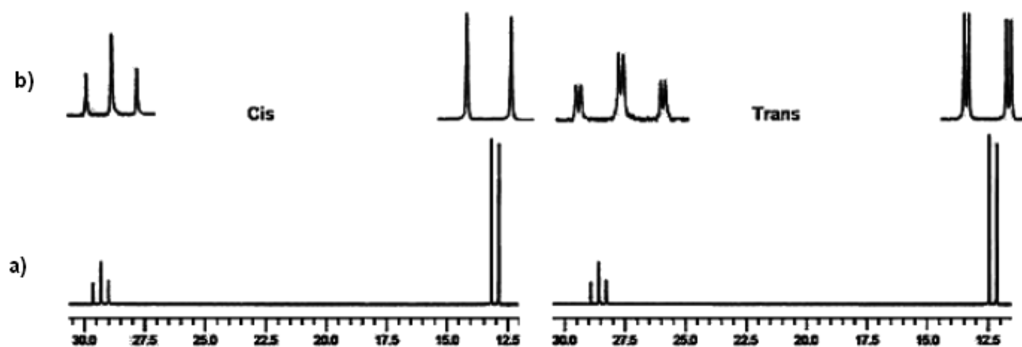


Figure 2. (a) ^1H -decoupled ^{31}P NMR spectra of cis and trans geometric isomers of 3d. (b) Addition of a CSA at ca. 10:1 mole ratio showing the doubling of signals characteristic of the racemate and meso isomers.

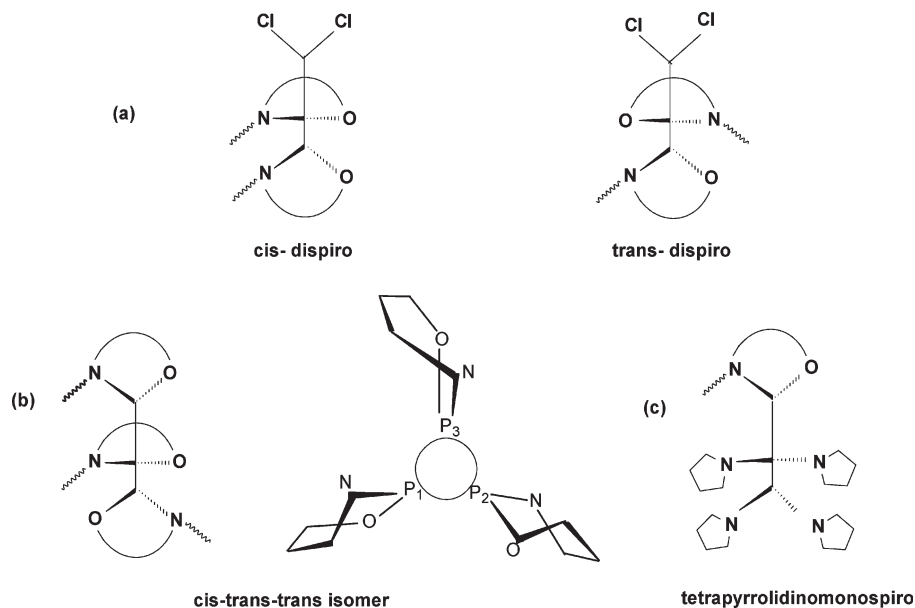


Figure 3. Possible geometric isomers of (a) di- (3a–3d) and (b) trispirocyclic (4a and 4b) phosphazenes and the propeller views of 4a and 4b. (c) Spatial view of tetrapyrrolidinomonospirophosphazenes (3f–3i).

The stereogenic properties of compounds 3a–3k are confirmed by ^{31}P NMR spectroscopy upon the addition of CSAs using the literature procedure.^{4b} Upon titration with CSAs, the chemical shifts change as a result of the equilibrium between the compound and its ligand-complexed form, and the changes (in ppb) at a mole ratio of CSA–compound of 10:1 are summarized in Table 6. In general, there are changes in both ^{31}P NMR chemical shifts (expressed in ppb) and magnitudes of $^2J_{\text{PP}}$. For instance, in the cis and trans isomers of 3d, there is no splitting of signals for the cis isomer, as was expected for a meso compound even upon the addition of a CSA up to a molar ratio of 50:1, but the signals of the trans isomer split into two peaks of equal intensities corresponding to the two enantiomers (Figure 2). The signals of the other trans isomers (3a–3c and 3e–3i) are also separated into two signals of equal intensities because of complexation with a CSA (Table 6). The examples are depicted in Figures 2 and 4 for 3b and 3j, respectively. The separations in the chemical shifts (in ppb) of the enantiomers at a mole ratio of CSA–compound of 10:1 are summarized separately in Table 6iii for the compounds. In general, there are greater changes in the separations of the enantiomers for compounds 3e–3h and 3i–3k than for compounds 3a–3d.

This is probably a result of better complexation of CSAs with compounds 3e–3h and 3i–3k having PNR and PORN groups, respectively, compared to compounds 3a–3d having PCl. In addition, the spin systems of trispiro derivatives (4a and 4b) are AB_2 , indicating that cis–trans–trans geometric isomers are formed. It is found that the orientations of the two *N*-alkyl (or aryl)spiro rings of 4a and 4b are the same, whereas the other is different; hence, the whole molecule looks similar to a propeller, where the chemical environment of P1 is different from that of P2 and P3, according to the ^{31}P NMR results, as was observed previously.^{14a} Moreover, the trans trispiro compounds, 3i–3k, also look similar to a propeller structure (Figure 3b).

In all of the spirophosphazene derivatives, the ^1H and ^{13}C NMR signals are assigned on the basis of chemical shifts, multiplicities, and coupling constants. The assignments are made unambiguously by the HETCOR corresponding to $^1J_{\text{CH}}$ between the C and H atoms (Table S1 in the Supporting Information). As an example, the HETCOR spectrum of 3j is depicted in Figure S1 in the Supporting Information. The benzylic OArCH_2N protons give rise to doublets for monospirophosphazenes (2a–2i) and multiplets for di- (3a–3i) and trispirophosphazenes (4a). The geminal OArCH_2N protons of 2a–2i are equivalent

Table 6. ^{31}P NMR Parameters of Compounds **3a–3k** and the Effect of a CSA on the ^{31}P NMR Chemical Shifts^a (X = Cl or pyr)

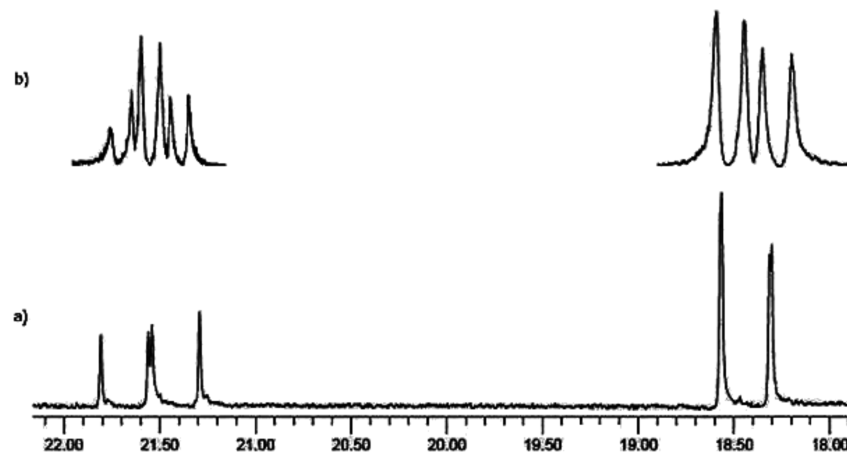
compound	δ (ppm)			$^2J_{\text{PP}}$ (Hz)
	PX ₂	P(OArN)	P(ORN)	
(i) ^{31}P NMR Chemical Shifts (ppm) and Geminal PNP Coupling Constants (Hz)				
3a	29.07	13.15		64.4
3b	28.20	11.70		65.3
3c	28.60	12.70		64.5
3d (cis) ^b	28.91	12.50		62.5
3d (trans)	28.60	12.30		63.8
3e	21.74	18.67		53.1
3f	21.67	17.37		53.3
3g	21.61	18.21		52.5
3h	21.78	18.14		52.1
3i		17.55	20.10	63.5
3j		17.43	19.93	63.3
3k		16.97	20.12	62.4
(ii) Effect of a CSA on the ^{31}P NMR Chemical Shifts (ppb) at a 10:1 Mole Ratio				
3a	−63	23		64.3
3b	130	−42.7		65.1
3c	62	38		64.3
3d	44	23		63.7
3e	−110	−113		52.1
3f	−160	−144		51.8
3g	−197	−372.5		50.7
3h	−160	−241		50.4
3i		−129.5	−81.5	66.3
3j		−353.5	−197	62.0
3k		−61	−123	61.1
(iii) Separation of the Enantiomeric Signals (ppb) at a 10:1 Mole Ratio of CSA—Molecule				
3a	39	27.5		
3b	101	54.5		
3c	36	32		
3d	36	31		
3e	94	132		
3f	256	130		
3g	150	227		
3h	174	166		
3i		73	13	
3j		155	166	
3k		88	40	

^a 202.38 MHz ^{31}P NMR measurements in CDCl_3 solutions at 293 K.^b As expected, no effect was observed up to a mole ratio of at least 50:1.

to each other and give doublets, and the average $^3J_{\text{PH}}$ value is 15.4 Hz. The geminal NCH_2Ar protons of **2a** and **2f** also give doublets, and the average $^3J_{\text{PH}}$ value is 9.9 Hz. The dispirophosphazenes (**3a–3k**) give highly complex ^1H NMR spectra because of the diastereotopic protons. The benzylic OArCH_2N protons of these compounds give rise to an ABX spin system because of the geminal proton–proton coupling and the vicinal coupling with the ^{31}P nucleus. The $^3J_{\text{PH}}$ values of OArCH_2N protons are between 6.7 and 10.0 Hz. In the ^1H NMR spectra of pyrrolidino-substituted mono- and dispirophosphazenes, the two pyrrolidino substituents bonded to the same P atom show two groups of NCH_2 (pyrr) signals with small separations (see the experimental part). The same situation is also observed for NCH_2CH_2 (pyrr) protons (Figure 3c).

The expected carbon signals are observed from the ^{13}C NMR spectra of all of the compounds. The NCH_2 signals of **2a**, **2f**, **2h**, **2i**, **3a**, **3e**, and **3g–3k** are confirmed by the HETCOR experiments, which are 46.00–46.38 ppm for NCH_2 (pyrr), 42.51–51.73 ppm for $\text{NCH}_2(\text{R})\text{Ar}$, and 41.22–50.01 ppm for OArCH_2 . In addition, the aromatic C atoms of the compounds are also determined by the HETCOR experiments (Figure S1 and Table S1 in the Supporting Information). The couplings $^3J_{\text{PC}2}$, $^2J_{\text{PC}3}$, and $^3J_{\text{PC}4}$ of mono- and dispirophosphazenes (except **3a**) give rise to doublets and triplets. The triplets possibly depend on the second-order effects, which are previously observed for analogous compounds.^{14a} In the ^{13}C NMR spectra of tetrapyrrolidinomonospirophosphazenes, the two pyrrolidino substituents bonded to the same P atom show two groups of NCH_2 (pyrr) and NCH_2CH_2 (pyrr) signals with small separations (see the experimental part; Figure 3c).

The FTIR spectra of all of the phosphazene derivatives show two medium-intensity absorption peaks at 3082–3057 and 3048–3026 cm^{-1} attributed to asymmetric and symmetric stretching vibrations of the Ar–H protons. They display intense bands between 1261 and 1163 cm^{-1} related to $\nu_{\text{P–N}}$ bonds of the phosphazene ring.^{14a,22} The characteristic ν_{NH} stretching bands of *N*-alkyl (or aryl)-*o*-hydroxybenzylamines disappear in the FTIR spectra of mono-, di-, and trispirophosphazenes. As expected, asymmetric and symmetric vibrations of ν_{PCL_2} arise for the partly substituted spirophosphazene derivatives (**2a**, **2b**, **2c**, **3a**, and **3b**) at 598–572 and 515–506 cm^{-1} .

**Figure 4.** (a) ^1H -decoupled ^{31}P NMR spectrum of compound **3j**. (b) Addition of a CSA at ca. 10:1 mole ratio showing the doubling of the number of signals, characteristic of a racemate isomer.

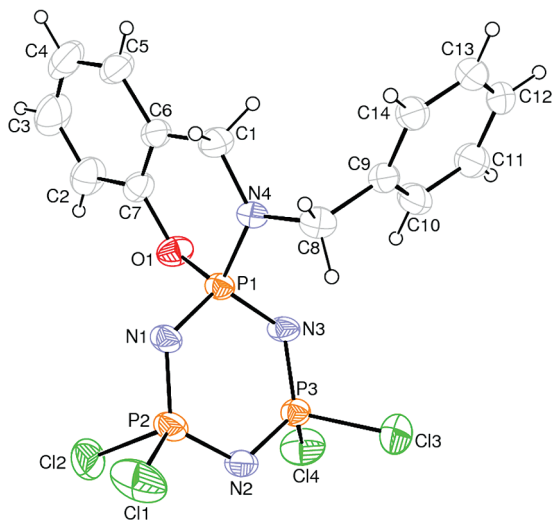


Figure 5. ORTEP-3²⁷ drawing of **2a** with the atom-numbering scheme. Displacement ellipsoids are drawn at the 30% probability level.

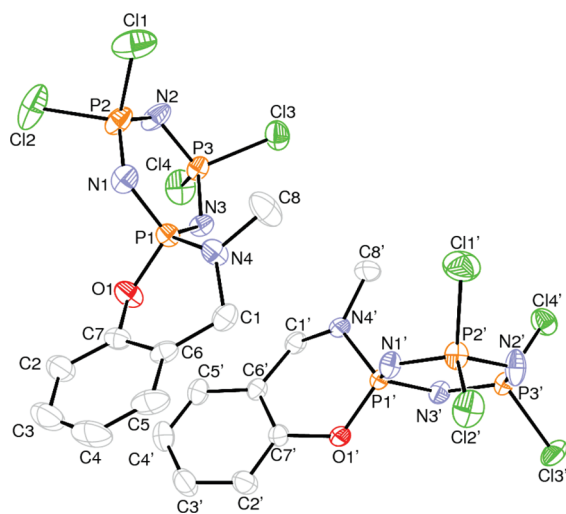


Figure 6. ORTEP-3²⁷ drawing of **2e** with the atom-numbering scheme. Displacement ellipsoids are drawn at the 30% probability level.

X-ray Structures of 2a, 2e, 2f, 3e, and 3f. The X-ray structural determinations of compounds **2a**, **2e**, **2f**, **3e**, and **3f** confirm the assignments of their structures from spectroscopic data. The asymmetric unit of **2e** contains two crystallographically independent molecules. The molecular structures of **2a**, **2e**, **2f**, **3e**, and **3f**, along with the atom-numbering schemes, are depicted in Figures 5–9, respectively. The phosphazene ring of **2e** is nearly planar [Figure S2a in the Supporting Information, $\varphi_2 = -79.7(5.3)^\circ$, $\theta_2 = 54.9(4.7)^\circ$], while **2a**, **2f**, **3e**, and **3f** are not planar but are in flattened-boat conformations [Figure S3a in the Supporting Information, $\varphi_2 = 96.4(1.6)^\circ$, $\theta_2 = 58.8(1.3)^\circ$; Figure S4a in the Supporting Information, $\varphi_2 = 73.6(0.4)^\circ$, $\theta_2 = 85.4(0.4)^\circ$; Figure S5a in the Supporting Information, $\varphi_2 = 59.9(0.6)^\circ$, $\theta_2 = 95.6(0.5)^\circ$; Figure S6a in the Supporting Information, $\varphi_2 = 147.8(2)^\circ$, $\theta_2 = 94.8(2)^\circ$] having total puckering amplitudes Q_T of 0.045(3) Å (for **2e**), 0.121(3) Å (for **2a**), 0.200(1) Å (for **2f**), 0.145(1) Å (for **3e**), and 0.345(1) Å (for **3f**) (twisted boat).²³

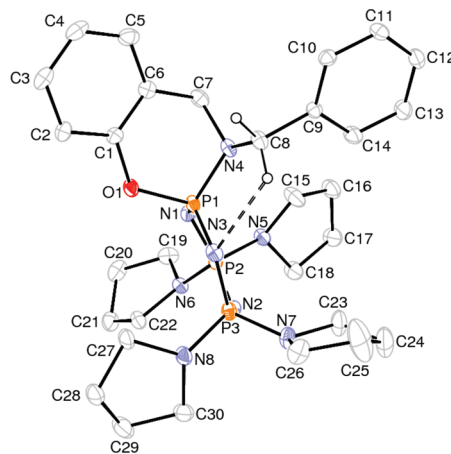


Figure 7. ORTEP-3²⁷ drawing of **2f** with the atom-numbering scheme. Displacement ellipsoids are drawn at the 30% probability level.

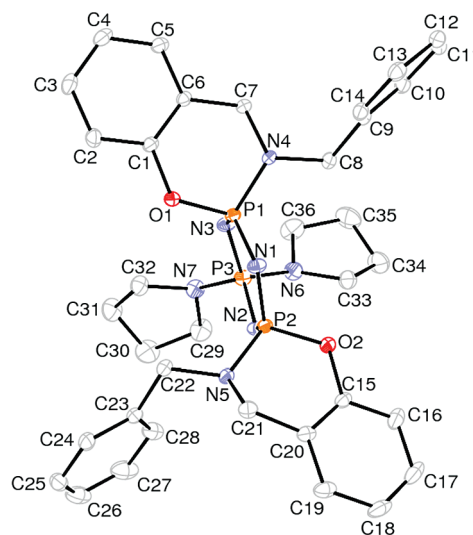


Figure 8. ORTEP-3²⁷ drawing of **3e** with the atom-numbering scheme. Displacement ellipsoids are drawn at the 30% probability level.

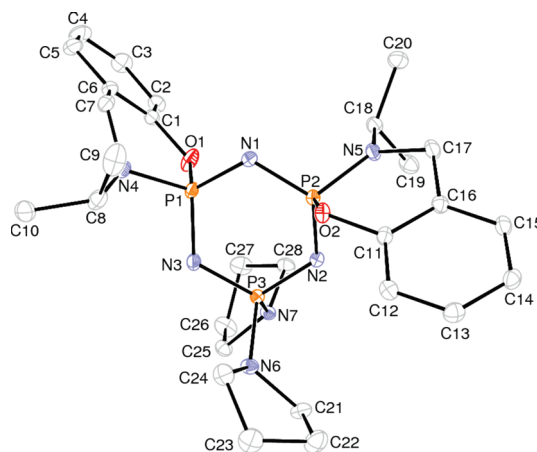


Figure 9. ORTEP-3²⁷ drawing of **3f** with the atom-numbering scheme. Displacement ellipsoids are drawn at the 30% probability level.

In monospirocyclic phosphazenes (**2a**, **2e**, and **2f**), the six-membered rings P1/O1/C1/C6/C7/N4 and P1'/O1'/C1'/C6'/C7'/N4' (for **2e**) are in boat conformations [Figure S3b in

(22) Carriedo, G. A.; Alonso, F. G.; Gonzalez, P. A.; Menendez, J. R. *J. Raman Spectrosc.* **1998**, 29, 327–330.

(23) Cremer, D.; Pople, J. A. *J. Am. Chem. Soc.* **1975**, 97(6), 1354–1358.

the Supporting Information, $Q_T = 0.431(4)$ Å, $\varphi_2 = -164.2(1)^\circ$, $\theta_2 = 128.4(1)^\circ$; Figure S2b in the Supporting Information, $Q_T = 0.534(6)$ Å, $\varphi_2 = 100.4(1)^\circ$, $\theta_2 = 36.6(1)^\circ$; Figure S4b in the Supporting Information, $\varphi_2 = 113.6(0.1)^\circ$, $\theta_2 = 56.1(0.1)^\circ$. In dispirocyclic phosphazenes, the six-membered rings P1/O1/C1/C6/C7/N4, P2/O2/C15/C20/C21/N5 and P1/O1/C1/C6/C7/N4, P2/O2/C11/C16/C17/N5 of **3e** and **3f**, respectively, are also in boat conformations [Figure S5b in the Supporting Information, $Q_T = 1.392(5)$ Å, $\varphi_2 = -122.2(1)^\circ$, $\theta_2 = 64.6(1)^\circ$; Figure S5b in the Supporting Information, $Q_T = 1.235(5)$ Å, $\varphi_2 = -74.1(1)^\circ$, $\theta_2 = 129.8(1)^\circ$; Figure S6b in the Supporting Information, $Q_T = 1.377(4)$ Å, $\varphi_2 = 117.9(1)^\circ$, $\theta_2 = 59.8(1)^\circ$; Figure S6b in the Supporting Information, $Q_T = 0.556(1)$ Å, $\varphi_2 = -5.9(7)^\circ$, $\theta_2 = 47.7(5)^\circ$].

In the phosphazene rings, the endocyclic PN bond lengths are in the ranges 1.548(3)–1.596(3) Å (for **2a**), 1.555(4)–1.588(4) and 1.550(4)–1.596(4) Å (for **2e**), 1.575(2)–1.610(2) Å (for **2f**), 1.577(2)–1.602(2) Å (for **3e**), and 1.571(2)–1.607(1) Å (for **3f**), and there are regular variations with the distances from P1: P1–N1 \approx P1–N3 > P2–N2 \approx P3–N2 > P2–N1 \approx P3–N3 for **2a** and **2e** and P1–N1 \approx P1–N3 < P2–N2 \approx P3–N2 < P2–N1 \approx P3–N3 for **2f**. On the other hand, the exocyclic PN bonds for spirorings are P1–N4 [1.613(3) Å] (for **2a**), P1–N4 [1.617(3) Å] and P1'–N4' [1.627(3) Å] (for **2e**), P1–N4 [1.662(2) Å] (for **2f**), P1–N4 [1.663(2) Å] and P2–N5 [1.648(2) Å] (for **3e**), and P1–N4 [1.649(2) Å] and P2–N5 [1.642(2) Å] (for **3f**) (Table 2). The average P–N bond lengths in the phosphazene rings are 1.570(4) and 1.573(4), 1.594(2), 1.589(2), and 1.593(1) Å, which are shorter than the average exocyclic P–N bonds of 1.622(3), 1.652(2), 1.650(2), and 1.649(2) Å for **2e**, **2f**, **3e**, and **3f**, respectively. In the phosphazenes, the P–N single and double bonds are generally in the ranges of 1.628–1.691 and 1.71–1.604 Å, respectively.²⁴ In recent years, natural bond orbital (NBO) and topological electron density analyses have been used to investigate the electronic structures of phosphazenes.²⁴ Phosphazene bonding alternatives are evaluated using NBO and negative hyperconjugation, and ionic bonding plays an important role for the P–N bond formation and is critical to the description of P–N bonding in these molecules. As a result of these investigations, ionic bonding is found to be the dominant feature, and the multiple-bond character can be attributed to the presence of negative hyperconjugation.^{24,25}

As can be seen from Table 2, in tetrachloro monospirocyclic phosphazenes (**2a** and **2e**), the endocyclic N1–P1–N3 (α) angles are narrowed, while the P1–N3–P3 (β) angles are considerably expanded with respect to the corresponding values in the “standard” compound, N₃P₃Cl₆. In N₃P₃Cl₆, the α and β angles are 118.3(2) and 121.4(3)°, respectively.²⁶ On the other hand, in tetrapyrrolidone monospirocyclic phosphazene (**2f**), the endocyclic N1–P1–N3 (α) angle is slightly expanded and the P1–N3–P3 (β) angle has almost the same value with the standard compound, whereas the P2–N2–P3 angle is highly expanded.

Table 7. Antimicrobial Activities of Compounds **2f**–**2i**, **3e**–**3i**, and **3k** on Bacterial and Yeast Cells (Inhibition Zone: mm)^a

test bacteria	compound												Keto
	2f	2g	2h	2i	3e	3f	3g	3h	3i	3k	Amp	C	
<i>S. aureus</i> ATCC 25923	19 ± 0	17.33 ± 0.58	34.5 ± 0.71	33.5 ± 0.71	11.5 ± 0.71	0.0	0.0	14.9 ± 0.17	0.0	18.67 ± 0.58	35 ± 0	28 ± 0	NS
<i>P. aeruginosa</i> ATCC 27853	0.0	18.5 ± 0.71	21.3 ± 0.71	24.33 ± 0.71	0.0	0.0	0.0	0.0	0.0	0.0	R	R	NS
<i>P. vulgaris</i> ATCC 8427	0.0	0.0	25.3 ± 0.71	0.0	0.0	0.0	0.0	0.0	0.0	23.33 ± 0.58	R	29 ± 0	NS
<i>E. coli</i> ATCC 35218	0.0	0.0	12.7 ± 0.58	13.5 ± 0.71	0.0	0.0	13.67 ± 0.58	0.0	0.0	0.0	R	10.0	NS
<i>E. coli</i> ATCC 25922	0.0	12.67 ± 0.58	23.67 ± 0.58	16.67 ± 0.71	0.0	0.0	0.0	18 ± 0	15.3 ± 0.58	0.0	20 ± 0	25 ± 0	NS
<i>E. faecalis</i> ATCC 29212	20 ± 2	20 ± 3	14.5 ± 0.71	11.5 ± 0.71	0.0	0.0	0.0	0.0	0.0	17 ± 0	29 ± 0	29 ± 0	NS
<i>B. cereus</i> NRRL-B-3711	18 ± 2	21 ± 2	27.3 ± 0.58	20 ± 1	12.67 ± 1.15	0.0	10.67 ± 0.58	17 ± 1	0.0	25 ± 1	10 ± 0	23 ± 0	NS
<i>B. subtilis</i> ATCC 6633	14.67 ± 0.58	17.33 ± 1.53	25 ± 2	17.5 ± 0.58	23.67 ± 0.58	0.0	14.5 ± 0.71	20 ± 1.41	15.67 ± 0.58	24.67 ± 1.15	30 ± 0	30.5 ± 0.7	NS
<i>C. albicans</i> ATCC 10231	13.3 ± 1.2	14 ± 0	11.5 ± 1.9	20 ± 1	0.0	0.0	0.0	0.0	0.0	0.0	NS	NS	30
<i>C. tropicalis</i> ATCC 13803	21.7 ± 1.2	14 ± 1.4	15.3 ± 2.9	17.5 ± 0.58	0.0	0.0	0.0	0.0	0.0	0.0	NS	NS	29

^a Antibiotics, Amp = ampicillin and C = chloramphenicol, Keto antifungal ketoconazole. Values represent averages ± standard deviations for triplicate experiments.

(24) Chaplin, A. B.; Harrison, J. A.; Dyson, P. J. *Inorg. Chem.* **2005**, *44*, 8407–8417.

(25) Krishnamurthy, S. S. *Phosphorus, Sulfur Silicon Relat. Elem.* **1994**, *87*, 101–111.

(26) Bullen, G. J. *J. Chem. Soc. A* **1971**, 1450–1453.

(27) Farrugia, L. J. *J. Appl. Crystallogr.* **1997**, *30*, 565–566.

Table 8. In Vitro Antimicrobial Activities of Compounds **2f–2i**, **3e–3i**, and **3k** (MIC Values)^a

microorganism names	MIC values									
	2f	2g	2h	2i	3e	3f	3g	3h	3i	3k
<i>S. aureus</i> ATCC 25923	156.25	19.53	9.76	19.53	312.5	NT	NT	78.12	NT	2500
<i>P. aeruginosa</i> ATCC 27853	NT	2500	625	41.66	NT	NT	NT	NT	NT	312.5
<i>P. vulgaris</i> ATCC 8427	NT	NT	19.53	NT	NT	NT	NT	NT	NT	NT
<i>E. coli</i> ATCC 35218	NT	NT	625	1250	NT	NT	NT	625	NT	NT
<i>E. coli</i> ATCC 25922	NT	41.66	625	41.66	NT	NT	312.5	NT	1250	NT
<i>E. faecalis</i> ATCC 292112	2500	19.53	2500	156.6	NT	NT	NT	NT	NT	2500
<i>B. cereus</i> NRRL-B-3711	156.25	2500	39.06	19.53	312.5	NT	312.5	19.53	NT	2500
<i>B. subtilis</i> ATCC 6633	625	2500	19.53	78.12	39.3	- NT	312.5	19.53	1250	2500
<i>C. albicans</i>	0.148	0.113	0.127	NT	NT	NT	NT	NT	NT	NT
<i>C. tropicalis</i>	0.170	0.133	0.068	NT	NT	NT	NT	NT	NT	NT

^a NT: not tested.

In dispirophosphazenes (**3e** and **3f**), the α angles [N1–P1–N3 117.8(1)° and N1–P2–N2 116.4(1)° for **3e** and N1–P1–N3 116.7(1)° and N1–P2–N2 116.6(1)° for **3f**] are slightly narrowed, while the β angles are slightly expanded only for **3e** with respect to the corresponding values in N₃P₃Cl₆. It is noteworthy that the endocyclic N–P–N angles of centered P atoms, which are bonded to pyrrolidino groups in **2f**, **3e**, and **3f**, are considerably narrowed [the average value of these angles is 115.0(1)°]. All of these results indicate that variations in the angles found in phosphazenes could be attributed to the substituent-dependent charge at the P centers and negative hyperconjugation.²⁴

The packing diagrams of **2a**, **2e**, **2f**, **3e**, and **3f** are given in Figures S2c–S6c in the Supporting Information, respectively. Compounds **2a**, **2f**, **3e**, and **3f** have intramolecular C–H···N hydrogen bonds (Table 3). In the crystal structure, compounds **2f** and **3e** have intermolecular hydrogen bonds, while compound **2f** also has an intermolecular C–H···O hydrogen bond (Table 3). In compound **3e**, intermolecular C–H···N hydrogen bonds (Table 3) link the molecules into infinite chains along the *c* axis (Figure S5c in the Supporting Information). In compound **2f**, intermolecular C–H···N and C–H···O hydrogen bonds (Table 3 and Figure S4c in the Supporting Information) link the molecules into a 2D network.

Antimicrobial Activities. A screening of antibacterial activities with eight bacteria [*Staphylococcus aureus* (ATCC 25923), *Pseudomonas aeruginosa* (ATCC 27853), *Escherichia coli* (ATCC 35218), *E. coli* (ATCC 25922), *Bacillus subtilis* (ATCC 29213), *B. cereus* (NRLL B-3008), *Proteus vulgaris* ATCC 8427, and *Enterobacter fecalis* (ATCC 292112)] was performed; the antifungal activity (*Candida albicans* and *C. tropicalis*) was also assessed, and the minimum inhibitory concentrations (MICs in mg/mL) were determined (Tables 7 and 8). MICs were found for **2f–2i**, **3e–3i**, and **3k**, ranging from 9.76 to 2500 mM. Compound **2h** demonstrates the most inhibitory activities with MIC values of 9.76 mM. Table 7 shows the antimicrobial effects of compounds **2f–2i**, **3e–3i**, and **3k**. All of the compounds (except **3f**) exhibit antimicrobial activity. Compounds **2f–2i**, **3e**, **3h**, and **3k** inhibit *S. aureus*. Compound **2h** is the most effective one, showing activity as much as control antibiotics. Compounds **2g** and **2h** reveal activities against *P. aeruginosa*. Only **2h** and **3k** reveal activities against *P. vulgaris*. Compounds **2h**, **2i**, and **3g** are active against *E. coli* (ATCC 35218). On the other hand, compounds **2g**, **2h**, **2i**, **3h**, and **3i** are active

against *E. coli* (ATCC 25922). Compounds **2f–2i** and **3k** are active against *E. faecalis*. Meanwhile, the compounds are very active against *B. cereus* (except **3f** and **3i**) and *B. subtilis* (except **3f**). In addition, **2f**, **2g**, and **2g** are also found to be active against yeast strain of *C. tropicalis* (ATCC 13803) and *C. albicans* (ATCC 10231). According to these findings, one can conclude that the compounds have strong antimicrobial effects on tested bacteria. The most susceptible strains are the Gram-positive *B. subtilis*, *B. cereus*, and *S. aureus*.

Consequently, pyrrolidine derivatives are widespread structural features of natural and biologically designed active molecules, and also they can be used for pharmaceutical purposes.²⁸ So, pyrrolidine is especially chosen as a substituent in this study. On the other hand, there are several studies about the antimicrobial/antibacterial activity of phosphazenes,¹⁰ but these compounds are not analogous compounds for comparison with pyrrolidino-substituted phosphazenes tested in this study. In addition, it is shown that the tetrapyrrolidinoferrocenylphosphazenes have antibacterial and antifungal activity.^{5c} However, pyrrolidino-substituted N/O spirocyclicphosphazenes (**2f–2i**, **3e–3i**, and **3k**) exhibited better activity with respect to the mono- and bisferrocenyltetrapyrrolidinophosphazenes.^{5c}

Interaction with pUC18 plasmid DNA and Restriction Enzyme Digestion. In order to find out whether **2f–2i**, **3e–3i**, and **3k** bind and induce conformational changes on the DNA helix, their capacities to remove and reverse the supercoiling of closed circular pUC18 DNA as assessed by electrophoretic mobility on agarose gels by incubating plasmid DNA with decreasing concentrations of the compounds were investigated. Figure 10 shows the electrophoretic mobility pattern of form I (ccc) and form II (oc) of pUC18 plasmid DNA after incubation at a range of concentrations with **2f–2i**, **3e–3i**, and **3k** for 24 h. In the electrophoretograms, the untreated pUC18 plasmid DNA is used as a control. Lines 2–6 refer to mixtures of DNA of varying concentrations of compounds ranging from 5000 to 156 μ M (line 2, 5000 μ M; line 3, 2500 μ M; line 4, 1250 μ M; line 5, 625 μ M; line 6, 312 μ M; line 7, 156 μ M). When pUC18 plasmid DNA interacts with decreasing concentrations of compounds **2f–2i**, **3e–3i**, and **3k**, a decrease in the mobility of form I is observed at two (three for **2h**, **2i**, **3f**, **3g**, **3i**, and **3k**) high concentrations.

(28) (a) Mitchell, R. E.; Teh, K. L. *Org. Biomol. Chem.* **2005**, *3*, 3540–3543. (b) Bellina, F.; Rossi, R. *Tetrahedron* **2006**, *62*, 7213–7256.

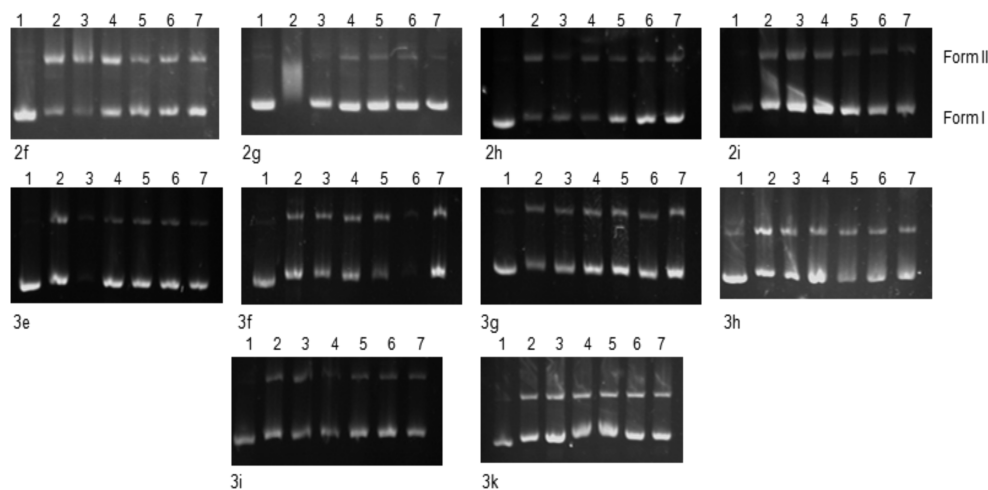


Figure 10. Gel electrophoretic mobility of pUC18 plasmid DNA when incubated with different concentrations of compounds **2f–2i**, **3e–3i**, and **3k**. Concentrations (in μM) are as follows: line 1, untreated pUC18 plasmid DNA; line 2, 5000; line 3, 2500; line 4, 1250; line 5, 625; line 6, 312; line 7, 156.

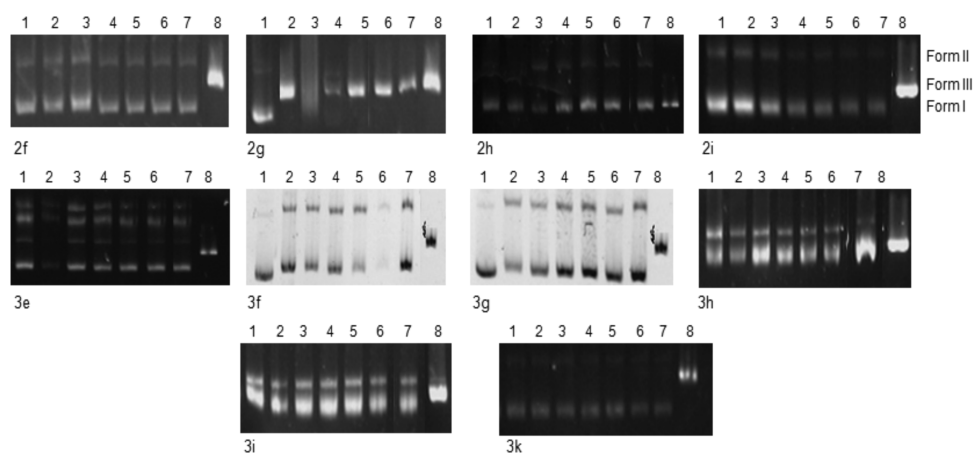


Figure 11. Electrophoretograms for the *Hind*III digested mixtures of pUC18 plasmid DNA after their treatment with various concentrations of compounds **2f–2i**, **3e–3i**, and **3k**. Concentrations (in μM) are as follows: line 1, untreated pUC18 plasmid DNA; line 2, 5000; line 3, 2500; line 4, 1250; line 5, 625; line 6, 312; line 7, 156; line 8, pUC18 plasmid DNA linearized by *Hind*III. Roman numerals I, II, and III indicate form I (covalently closed circular), form II (open circular), and form III (linear) plasmids, respectively.

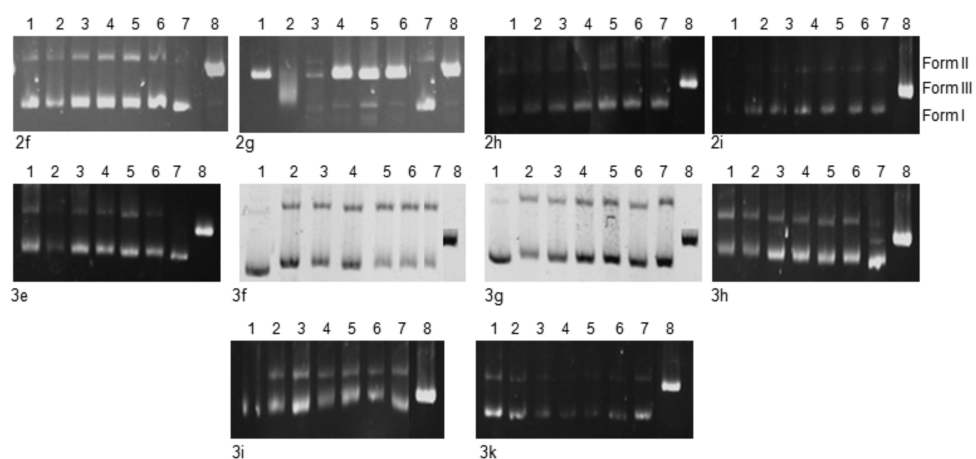


Figure 12. Electrophoretograms for the *Bam*HI digested mixtures of pUC18 plasmid DNA after their treatment with various concentrations of compounds **2f–2i**, **3e–3i**, and **3k**. Concentrations (in μM) are as follows: line 1, untreated pUC18 plasmid DNA; line 2, 5000; line 3, 2500; line 4, 1250; line 5, 625; line 6, 312; line 7, 156; line 8, pUC18 plasmid DNA linearized by *Bam*H. Roman numerals I, II, and III indicate form I (covalently closed circular), form II (open circular), and form III (linear) plasmids, respectively.

Compounds **2f**, **2h**, **3g**, and **3i** decrease the intensities of the form I bands. The increase in the intensities of the form I band is observed for **2i** at three high concentra-

tions. Compound **2g** shows a coalescence point and indicates a strong unwinding of form I. In general, compounds are active at three high concentrations.

In order to find out whether compounds, **2f–2i**, **3e–3i**, and **3k** show affinity toward guanine–guanine and/or adenine–adenine nucleotides of DNA, restriction analysis of the compound–DNA adducts digested with *Hind*III and *Bam*HI enzymes was performed. *Hind*III and *Bam*HI enzymes bind at sites 5'-A/AGCTT-3' and 5'-G/GATCC-3' of DNA, cleave these sequences, and convert forms I and II DNA to the linear form III DNA. All of the compounds, except **2g**, prevent digestion with *Hind*III and *Bam*HI enzymes; this may be due to the binding of the compounds to the DNA (Figures 11 and 12).

Conclusions

The spirocyclic phosphazene derivatives containing 1,3,2-oxazaphosphorine rings are very limited in the literature. In this study, new mono- (**2a–2i**), di- (**3a–3k**), and trispirocyclic (**4a–4d**) phosphazene derivatives with chiral properties (except monospirocyclic ones) are obtained. Compounds **3a–3h** have two stereogenic P atoms. They are expected to be in the cis (meso) and trans (racemic) geometric isomers. Only the trans isomers of **3a–3d** are isolated and reacted with pyrrolidine and sodium 3-amino-1-propanoxide to give **3e–3k**. In addition, the enantiomers of chiral phosphazenes are determined by changes in the ^{31}P NMR spectra upon the addition of CSAs. In general, there are changes in both δP shifts and $^2J_{\text{PP}}$ coupling constants. In the trans trispirocyclic compounds (**3i–3k**), there are three stereogenic P atoms. The molecular structures of **3i–3k**, **4a**, and **4b** look similar to a propeller, where the chemical environment of P1 is different

from that of P2 and P3. In addition, **4a** and **4b** exist as cis–trans–trans geometric isomers. Among the phosphazenes tested, all of the compounds (except **3f**) have strong antimicrobial activities. MICs determined for these compounds range from 9.76 to 2500 mM. Compound **2h** demonstrates the most inhibitory activities, with MICs ranging from 9.76 to 2500 mM. Biological activity studies suggest that they may serve as potential candidates of new antimicrobial agents. On the other hand, compound–DNA interaction studies show that the compounds cause changes in the mobility of the form I band of plasmid DNA. The compounds, except **2g**, are found to be similar in their ability to cause unwinding of supercoiled form I pUC18 plasmid DNA and prevent *Bam*HI and *Hind*III digestion, in their activity and binding with DNA.

Acknowledgment. The authors acknowledge the Scientific and Technical Research Council of Turkey (Grant 106T503). T.H. is indebted to Hacettepe University, Scientific Researchs Unit (Grant 02 02 602 002) for financial support.

Supporting Information Available: Listings of the HETCOR spectrum of **3j** (Figure S1), ring conformations, crystal packing diagrams (Figures S2–S6), and X-ray crystallographic files in CIF format for compounds **2a**, **2e**, **2f**, **3e**, and **3f**, 2D ^1H – ^{13}C HETCOR correlation for compound **3j** (Table S1), antimicrobial activities (section S1), and DNA and compound interactions (section S2). This material is available free of charge via the Internet at <http://pubs.acs.org>.